Approximate Capacitance Formulas for Electrically Small Tubular Monopole Antennas

David F. Rivera
Dr. John P. Casey
Submarine Electromagnetic Systems Department

DTIC
SELECTED
DEC 1 1 1995
B
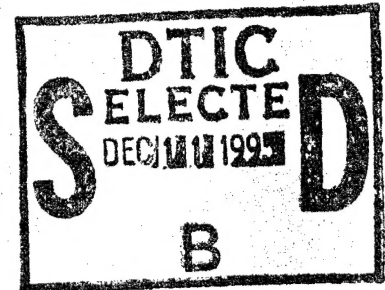
19951207 039

Naval Undersea Warfare Center Division
Newport, Rhode Island

Approved for public release; distribution is unlimited.

Preface

Acknowledgments

Reviewed and Approved: 19 January 1995

Daniel M. Viccione

D. M. Viccione
Head, Submarine Electromagnetic Systems Department

REPORT DOCUMENTATION PAGE

Form Approved
OMB No. 0704-0188

1. AGENCY USE ONLY (Leave Blank)	2. REPORT DATE 19 January 95	3. REPORT TYPE AND DATES COVERED Final

4. TITLE AND SUBTITLE

Approximate Capacitance Formulas for Electrically Small Tubular Monopole Antennas

5. FUNDING NUMBERS

6. AUTHOR(S)

David F. Rivera, Dr. John P. Casey

7. PERFORMING ORGANIZATION NAME(S) AND ADDRESS(ES)

Naval Undersea Warfare Center Detachment
39 Smith Street
New London, Connecticut 06320-5594

8. PERFORMING ORGANIZATION REPORT NUMBER

TR 10,817

9. SPONSORING/MONITORING AGENCY NAME(S) AND ADDRESS(ES)

Office of Naval Research
Code 313
Washington, DC

10. SPONSORING/MONITORING AGENCY REPORT NUMBER

11. SUPPLEMENTARY NOTES

12a. DISTRIBUTION/AVAILABILITY STATEMENT

Approved for public release; distribution unlimited

12b. DISTRIBUTION CODE

13. ABSTRACT (Maximum 200 words)

Analytical approximations have been developed to compute the capacitance of electrically small tubular monopole antennas. The expressions developed are algebraically simple, facilitating manual calculations and rapid iteration of designs when used in a computer program. Plots are given of the accuracy of previous expressions and the approximations developed herein as a function of the arguments. It is shown that the approximations are sufficiently accurate, making them useful as tools to aid in the design of electrically short cylindrical monopoles over a wide range of heights, lengths, and diameters.

14. SUBJECT TERMS

Electrically small antennas
Monopoles
Capacitance
Moment Method

15. NUMBER OF PAGES

70

16. PRICE CODE

17. SECURITY CLASSIFICATION OF REPORT UNCLASSIFIED	18. SECURITY CLASSIFICATION OF THIS PAGE UNCLASSIFIED	19. SECURITY CLASSIFICATION OF ABSTRACT UNCLASSIFIED	20. LIMITATION OF ABSTRACT UNLIMITED

TABLE OF CONTENTS

LIST OF ILLUSTRATIONS

LIST OF ILLUSTRATIONS (Cont'd)

iii

LIST OF TABLES

1. BACKGROUND

A monopole antenna is said to be electrically small when its largest physical dimension is much smaller than the wavelength at which it operates. These antennas are commonly found in the portion of the radio frequency spectrum spanning from VLF to MF (3 - 3000 kHz). At these frequencies, such antennas are employed in maritime communications, air and coastal navigation, as well as local broadcasting [1-3].

The input impedance of an electrically small monopole can be represented by a series circuit comprising a resistance R and a capacitive reactance $-1/\omega C$, such that $R \ll 1/\omega C$ [1]. The series resistance is the sum of the radiation resistance and other resistances attributed to ohmic (dissipative) losses. The monopole capacitance C can be derived using electrostatic methods and depends on three principal quantities: its diameter d, length l, and height h measured from the bottom of the antenna to the ground plane. Such an arrangement is shown in Fig. 1(a), where the wall thickness t of the tube is assumed to be very thin compared to the diameter.

In the design of such an antenna, the goal is to minimize the capacitive reactance and maximize the radiation resistance. Achieving this goal usually involves an increase in the effective antenna radius and/or length by using, for example, a folded monopole with one or more input impedance transforming elements [4-5], a capacitive top load [6], or both [7]. In addition, the capacitance of the electrically small tubular monopole is extremely important for the determination of the antenna's power handling ability (P_{max}) and the bandwidth-radiation efficiency product (BW·η) [8-9] given as follows:

$$P_{max} = \frac{640\,\pi^4\,f^4\,V_b^2\,h_e^2\,C^2}{c^2} \qquad (1)$$

$$BW\cdot\eta = \frac{320\,\pi^3\,f^4\,h_e^2\,C}{c^2} \qquad (2)$$

where

> h_e = effective height,
> f = frequency,
> C = antenna capacitance,
> V_b = maximum allowable base voltage before breakdown,
> c = velocity of light.

In designing electrically small monopole antennas, the engineer must be concerned with these antenna performance parameters as well as any number of mechanical requirements that may be

imposed. The complete design process is therefore seen as highly iterative, involving the examination of achievable electrical and mechanical properties until a satisfactory solution is obtained.

A precise determination of the input capacitance of an electrically small antenna may be obtained through the solution of the potential integral equation for the unknown charge distribution using the method of moments [10]. However, such a numerical method does not lend itself to rapid iterative design calculations.

Approximate analytical expressions for the input capacitance are available for two extreme cases, i.e., for a thin wire ($d/l \ll 1$) and for a thick tube [($d/l \gg 1$), with vanishingly thin walls], each above a ground plane. The capacitance of a thin vertical wire above a ground plane was determined by Grover [11]. By the use of a method originally proposed by Howe [12], Grover obtained an analytical expression for the capacitance by assuming that the charge distribution along the antenna was constant. The converse problem, that of the capacitance of a thick tubular monopole, was solved by Casey and Bansal [13]. Through modification of the per-unit length capacitance of a coplanar stripline given by Hanna [14], Casey and Bansal obtained an expression for the equivalent tubular monopole in terms of elliptic integrals.

Although the expressions cited above have been experimentally validated for some specific monopole dimensions, the extent of diameters, lengths and ground plane separations for which they are accurate has been unknown. When used for the rapid iteration of a design, capacitance values obtained with the known expressions will be of questionable value. A determination of the regions of validity of the existing tubular monopole capacitance formulas is therefore necessary for their successful implementation. It is the purpose of this report to summarize the results of such an investigation and present new capacitance formulas for parameter ranges not covered by the existing expressions. The end result of this study is a collection of formulas that, taken together, extend the parameter range so that the computation of capacitance can be facilitated with reasonable accuracy for almost all design situations considered in practice.

2. APPROACH

The range of validity of Grover's formula for the capacitance of a thin wire or tubular monopole and the range of validity of the thick tubular monopole formula developed by Casey and Bansal will be examined by comparison with results obtained by a method of moments solution [15]. (It may be noted that the method of moments results have been experimentally verified [13,15].) The range of validity is defined here as that area where the formula agrees to within 10% of the method of moments results. A 10% error region is chosen since influences such as the antenna's proximity to other objects or irregularities in the ground plane may introduce variations

of this magnitude in the observed capacitance.

With the regions of validity defined for the existing capacitance formulas, additional expressions will be presented that are suitable for parameter ranges not covered by the existing equations. An error analysis of these new capacitance formulas will follow.

Tubular monopoles can be fed in a variety of ways, two of which are shown in Fig. 2. In general, the monopole capacitance is approximately the sum of the individual capacitances of both the tube and the feed sections. The capacitance of a thin feed wire (Fig. 2(a)) is normally much smaller than the tube capacitance and can be neglected. In contrast, the capacitance of the conical feed as shown in Fig. 2(b) must usually be accounted for. Information on the computation of the illustrated feed capacitances can be found in [16-17]. In the case where there is a plate attached to both the feed wire and the lower end of the tube, a first order estimate of the monopole capacitance is the sum of the individual capacitances. Information on the capacitance of a flat plate is given in [18]. The effects of top loading and base supports may be treated by techniques given by Belrose [3] and are not considered here. Appendix A provides a listing of capacitance formulas for various tubular monopole feeds along with other effects including the finite wall thickness of the tube.

3. EXISTING APPROXIMATIONS AND THEIR REGIONS OF VALIDITY

3.1. Thin Tubes

Consider the tubular monopole and associated coordinate system as described in Fig. 1(b). The electrostatic potential at any point along the tube surface due to an axisymmetric surface charge density $\sigma(z) = q(z)/\pi d$ induced on the tube is found by summing the contribution of the charge along the cylinder as [15]

$$V(z) = \frac{1}{4\pi\varepsilon_0} \int_h^{h+l} q(z') \left[K(z - z') - K(z + z') \right] dz' \ , \quad z \in (h, h+l) \tag{3}$$

where

$$K(\zeta) = \frac{1}{2\pi} \int_{-\pi}^{\pi} \frac{1}{\sqrt{\zeta^2 + d^2 \sin^2 \frac{\varphi'}{2}}} d\varphi' \quad . \tag{4}$$

In (3), q(z) is the charge per unit length while K(z - z') and K(z + z') are the kernels associated with the tube and its image, respectively. Note that a cylindrical coordinate system is used in (3) and (4), where φ denotes the azimuthal variable while the primed and unprimed coordinates refer to the source and observation points, respectively. Since the tube is highly conducting, it will be an

equipotential surface with $V(z) = V$ (a constant), where V is the potential of the tube with respect to ground.

The charge distribution that results from solving the integral equation (3) when the potential $V(z)$ is constant was calculated using the method of moments. A representative charge distribution is shown in Fig. 3. The charge density is fairly constant across the interior of the interval $(h,h+l)$ with singularities at the edges. The charge density is asymmetric about its midpoint as more charge accumulates on the ground plane side of the tube. This asymmetry becomes more apparent as the separation h decreases.

For thin tubes or wires ($d/l \ll 1$), Grover derived a formula for the capacitance of a monopole using Howe's method of approximation. In Howe's approximation (contrary to the physical reality) the total charge Q is assumed to be uniformly distributed over the length of the tube, thereby reducing (3) to

$$V(z) \cong \frac{Q}{4\pi\varepsilon_0 l} \int_h^{h+l} \left[K(z - z') - K(z + z') \right] dz' \ , \quad z \in (h,h+l) \ . \tag{5}$$

Note that the potential becomes a function of position along the tube. The capacitance is estimated as $C = Q/V_{av}$, where V_{av} is the average of $V(z)$ over $(h,h+l)$. Upon application of the above procedure followed by further simplification under the condition $d/l \ll 1$, Grover derived the following [11]:

$$C = \frac{2\pi\varepsilon_0 l}{\ln\left(\frac{2}{D}\right) - \gamma} \tag{6}$$

where $D = d/l$ and γ is defined as

$$\gamma = 1 + (1 + H) \ln (1 + H) - (1 + 2H) \ln (1 + 2H) + H \ln (4H) \tag{7}$$

where $H = h/l$. For simplicity, we will adopt the symbols D and H throughout the remainder of the report. Note that as $H \to \infty$, $\gamma \to 1 - \ln 2$ and Grover's formula yields the capacitance of a tube of length l in free space. However, as $H \to 0$, $\gamma \to 1$ and the capacitance does not diverge as expected, but instead approaches a constant.

A contour plot illustrating the percentage error of the capacitance per unit length of Grover's formula based on a comparison with a method of moments solution is given in Fig. 4 for $-4 \leq \log_{10}(H) \leq 1$ and $-3 \leq \log_{10}(D) \leq 0$. Grover's formula produces data within 10% of the moment-method results for $D \leq 0.008$ over the entire range of ground plane separations considered in this study. Although Grover's formula does not produce the correct result in the limiting case as $H \to 0$, it still yields sufficiently accurate data for the small values of H plotted with $D \leq 0.008$. As H

4

increases, Grover's formula generally improves until H = 0.04, where the contours begin to level off. Grover's formula, though not based on assumptions that accurately describe the charge and voltage distributions, provides a useful expression for the capacitance within the regions stated above.

The method of moments code that was used in this comparison is based on the solution of the potential integral equation (3) for the unknown charge density q(z). The numerical procedure employs pulse expansion functions and point matching. The kernel K(ζ) of the potential integral equation, defined in (4), is expressible in terms of the complete elliptic integral of the first kind, for which polynomial approximations exist [19]. For each data point computed, a sufficient number of basis functions was chosen to ensure convergence to at least three significant figures. The details of this program are provided in [15]. An examination of the numerical convergence of the method of moments algorithm used in this report is given in Appendix C.

3.2. Thick Tubes

Casey and Bansal [13] developed an expression for the capacitance of a tubular monopole through comparison with a formula for the capacitance of a coplanar stripline. Figure 5 illustrates the approximate equivalence utilized in this development. The expression is based on a conformal mapping and is given by

$$C = 2\pi\varepsilon_o d \frac{K(k')}{K(k)} \quad , \tag{8}$$

where

$$k = \frac{H}{1 + H} \tag{9}$$

and

$$k' = \sqrt{1 - k^2} \quad . \tag{10}$$

K(k) is the complete elliptic integral of the first kind. An accurate approximation for the ratio of the complete elliptic integrals in (8) is given as

$$\frac{K(k')}{K(k)} \cong \frac{2}{\pi} \cosh^{-1} \left[\frac{1 + k'}{k} + \frac{k \sqrt[4]{k'}}{4 \left(1 + k' \right)} \right] \quad . \tag{11}$$

The development and error analysis of (11) are given in Appendix B. Equation (8) will be referred to as the conformal mapping approximation (CMA) formula. Figure 6 illustrates a comparison between the CMA formula and experimental data for tubes of various dimensions and ground plane separations. It can be seen that the data are in good agreement.

A contour plot illustrating the percentage error of the capacitance per unit length of the CMA formula based on a comparison with the method of moments solution is given in Fig. 7 for $-4 \leq \log_{10}(H) \leq 1$ and $-2 \leq \log_{10}(D) \leq 3$. The CMA formula produces data within 10% of the method of moments results for thick monopoles within the region $D \geq 2/\ln[1 + (3/H)]$ and $H \geq 10^{-4}$. The former boundary was obtained by fitting a curve to the calculated boundary points. For sufficiently thick monopoles (i.e., $D > 10$), the error contours are nearly vertical lines (independent of D) since the differences in the electric field lines associated with the monopole and the corresponding stripline change very little with increasing tube diameter.

For $D > 10$, the error in the CMA formula slowly oscillates with separation from the ground plane over the entire range of H shown, and then monotonically increases for large H (not shown in Fig. 7). The increasing error in the CMA formula for large H occurs because the electric field lines extending from the inside surface of the tube are no longer the same shape as those extending from the outside surface. The required symmetry is preserved for greater ground-plane separations when the diameter of the tube is larger.

4. EXTENSION OF GROVER'S FORMULA

As discussed in the previous section, Grover's capacitance formula, based on Howe's method of approximation, is valid only for thin tubes while the CMA formula is valid for thick tubes. In an attempt to bridge the gap between the CMA and Grover formulas, the authors have extended the Grover formula to include fewer restrictions on D and H. An outline of the development of this formula along with results are given below.

Consider again expression (3) for the electrostatic potential along the surface of the tubular monopole due to a surface charge density $q(z)/\pi d$. Since the surface charge distribution is axisymmetric, the kernel $K(\zeta)$ defined in (4) may be approximated as

$$K(\zeta) \cong \frac{1}{\sqrt{\zeta^2 + \left(\frac{d}{2}\right)^2}} \ . \tag{12}$$

The above approximation, sometimes referred to as the reduced kernel, is applicable to thin tubes. Next we will apply Howe's approximation to the determination of the tubular monopole capacitance using the reduced kernel (12). The substitution of (12) into the potential integral (5) yields

$$V(z) \cong \frac{Q}{4\pi\varepsilon_o l} \int_h^{h+l} \left[\frac{1}{\sqrt{(z-z')^2 + (d/2)^2}} - \frac{1}{\sqrt{(z+z')^2 + (d/2)^2}} \right] dz \ , \ z \in (h, h+l) \qquad (13)$$

where Q is the total charge along the monopole. The evaluation of the integral in (13) yields

$$V(z) = \frac{Q}{4\pi\varepsilon_o l} \left\{ \ln\left[\frac{(z-h) + \sqrt{(z-h)^2 + (d/2)^2}}{(z-h-l) + \sqrt{(z-h-l)^2 + (d/2)^2}} \right] - \ln\left[\frac{(z+h+l) + \sqrt{(z+h+l)^2 + (d/2)^2}}{(z+h) + \sqrt{(z+h)^2 + (d/2)^2}} \right] \right\}$$

$$= \frac{Q}{4\pi\varepsilon_o l} \left\{ \sinh^{-1}\left(\frac{z-h}{d/2}\right) - \sinh^{-1}\left(\frac{z-h-l}{d/2}\right) - \sinh^{-1}\left(\frac{z+h+l}{d/2}\right) + \sinh^{-1}\left(\frac{z+h}{d/2}\right) \right\} \ .. \qquad (14)$$

Note that the final result follows since $\sinh^{-1}(x) = \ln(x + \sqrt{x^2 + 1})$. The average potential along the monopole is

$$V_{av} = \frac{1}{l} \int_h^{h+l} V(z) \ dz = \frac{Q}{2\pi\varepsilon_o l} \Psi(D,H) \ , \qquad (15)$$

where

$$\Psi(D,H) = \sinh^{-1}\left(\frac{2}{D}\right) - (1+H)\sinh^{-1}\left(\frac{4(1+H)}{D}\right) + (1+2H)\sinh^{-1}\left(\frac{2(1+2H)}{D}\right) - H\sinh^{-1}\left(\frac{4H}{D}\right)$$

$$+ \frac{D}{2} - \sqrt{1 + (D/2)^2} + \sqrt{H^2 + (D/4)^2} + \sqrt{(1+H)^2 + (D/4)^2} - \sqrt{(1+2H)^2 + (D/4)^2} \qquad (16)$$

with $D = d/l$ and $H = h/l$. The monopole capacitance is given by

$$C = \frac{Q}{V_{av}} = \frac{2\pi\varepsilon_o l}{\Psi(D,H)} \ . \qquad (17)$$

The extended Grover formula (17) is considerably more involved than Grover's formula (6). For the case of very thin tubes (D « 1) it can be shown that (17) reduces to (6).

A contour plot illustrating the percentage error of the capacitance per unit length of the extended Grover formula based on a comparison with the method of moments data is given in Fig. 8 for -4 $\leq \log_{10}(H) \leq 1$ and $-3 \leq \log_{10}(D) \leq 1$. A comparison of Figs. 4 and 8 indicates that the extended Grover formula provides a small improvement over Grover's formula for $H \geq 0.1$. More specifically, for $H \geq 0.1$, one is able to model monopoles (within 10% of the moment-method data) with the extended Grover formula for $D \leq 1.0$ in comparison to $D \leq 0.35$ with Grover's formula. Both Grover's formula and the extended Grover formula produce similar results for H <

0.1.

The inability of the extended Grover formula to model much thicker tubes is attributed to the approximate reduced kernel (12) which is valid only for thin tubes. In addition, the Howe approximation limits the ability of the extended Grover's formula to yield an improvement over Grover's formula for small relative ground plane separations (H < 0.1). In conclusion, with the added number of terms involved, the extended Grover formula does not appear to offer a significant improvement over Grover's result.

5. APPROXIMATE EXPRESSION FOR INTERMEDIATE PARAMETER RANGE

In the previous sections, the capacitance formulas presented were for cases in which the antenna is considered thin or thick. As a result, an expression was sought that produced a fit to the capacitance data obtained from a moment-method calculation for regions not accurately represented by either the CMA or Grover's formula. The area of interest is a rectangular region with boundaries defined by $-2.5 \leq \log_{10}(D) \leq 1$ and $-4 \leq \log_{10}(H) \leq 1$. This region was chosen since it was considered to cover most of the areas where the existing formulas fail and provides a sufficient amount of overlap. A suitable form for an expression that adequately describes the capacitance variation with variables D and H is arrived at by the observations that follow.

To be useful, the desired capacitance expression must possess the limiting behaviors described below.

i) Tube close to the groundplane

In this region, the capacitance can be represented by the behavior of the CMA (8) for $H \rightarrow 0$. Here one can utilize the asymptotic representation for the ratio of elliptic integrals $K(k')/K(k)$ for small modulus k [20]:

$$\lim_{k \rightarrow 0} \left[\frac{K(k')}{K(k)} \right] \rightarrow \frac{2}{\pi} \ln\left(\frac{4}{k}\right) . \tag{18}$$

The substitution of (9) into (18), followed by the application of (8) leads to the limiting behavior of the normalized capacitance, given as

$$\frac{C}{\varepsilon_o l} \rightarrow 8D \ln(2) + 4D \ln\left(1 + \frac{1}{H} \right) , \ H \rightarrow 0. \tag{19}$$

Grover's expression (6) was not considered for vanishingly small H because it is only a function of D in this case.

ii) Tube far from the groundplane

In this region, the capacitance of the tube is independent of the height above the groundplane and

$$\frac{C}{\varepsilon_o l} \to \alpha(D) \ , \ H \to \infty. \tag{20}$$

In (20), $\alpha(D)$ is a function determined from the method of moments data.

Expressions (19) and (20) can be combined to yield a function possessing the limiting behaviors described above, as

$$\frac{C}{\varepsilon_o l} = \alpha(D) + 4D \ln\left[1 + \frac{\beta(D)}{H}\right] . \tag{21}$$

In (21), the function $\alpha(D)$ replaces $8D \ln(2)$ and $\beta(D)$ is introduced in order to allow the second term to remain valid for large values of D and H. The factor 4D in the second term has been retained since it is valid for small values of H.

The normalized tubular capacitance, $C/(\varepsilon_o l)$, was computed using the method of moments for the parameter range of $-2.5 \le \log_{10}(D) \le 1$ and $-4 \le \log_{10}(H) \le 1$. A plot of $C/(\varepsilon_o l)$ as a function of D and H resulting from the computation in this range is shown in Fig. 9. From the data, the functions $\alpha(D)$ and $\beta(D)$ were determined by nonlinear regression, with the following forms:

$$\alpha(D) \cong \frac{7}{\ln\left(1 + \frac{2}{D}\right)} \ , \ \beta(D) \cong \frac{1 + 30D + 124D^2}{70D(D+2)} . \tag{22}$$

The substitution of the expressions in (22) into (21) results in an expression for the normalized capacitance valid in the desired range, given by

$$\frac{C}{\varepsilon_o l} \cong \frac{7}{\ln\left(1 + \frac{2}{D}\right)} + 4D \ln\left\{1 + \left[\frac{1 + 30D + 124D^2}{70HD(D+2)}\right]\right\} . \tag{23}$$

Equation (23) will be referred to as the approximate capacitance formula (ACF). An error contour plot of (23) is shown in Fig. 10. The plot indicates that the error in the ACF is within 10% of the method of moments results over virtually the entire region shown. In particular, the error in the ACF is less than 3% for $H < 0.1$ and generally increases with H. The ACF is a simple formula that provides an accurate estimate of capacitance over the designated region of interest.

6. DISCUSSION OF RESULTS

Table I summarizes the ranges where the capacitance formulas discussed in this report are within 10% of the method of moments results. The four formulas presented here are seen to be accurate for wide ranges in the parameters D and H. In the case of the CMA formula, the lower boundary defining the region in which the accuracy is better than 10% is given as an approximate function of H.

Although in practice monopoles are mounted close to the ground plane (H « 1), we observe that the capacitance formulas are accurate over a wide range of H. Undoubtedly, the use of a tubular monopole far removed from the ground is unlikely in most applications. In order to gauge the utility of these formulas for large separations from the ground, it would be instructive to do a simple comparison against known capacitance formulas for tubes of arbitrary diameters and lengths in free space.

For the investigation of tubular monopole capacitance formulas for large H, we define a ratio R as

$$R = \frac{C_{gp}}{C_{fs}} = 1 + \delta \quad , \tag{24}$$

where C_{gp} and C_{fs} refer to the capacitances of a tube above a ground plane and in free space, respectively, and δ is the difference in the capacitances relative to the free space value. As H becomes large, $R \to 1$ (i.e., $\delta \to 0$). A "free space" boundary can be defined as the normalized height H that corresponds to a predetermined small value of δ (i.e., δ « 1). A mathematical fit describing the boundary for the height-to-length ratio H_{fsb} along which $\delta = 0.01$ is given by

$$H_{fsb} \cong \frac{35}{\ln\left(1 + \frac{2}{D}\right)} \quad , \tag{25}$$

applicable for $D \geq 10^{-3}$. Expression (25), obtained from an approximate fit to the method of moments data, essentially separates two regions; for $H < H_{fsb}$ the monopole formulas are appropriate, while for $H > H_{fsb}$ the free space expressions apply.

Expressions for the free space capacitance of thin and thick tubes have been derived by Howe [12] and Butler [21], respectively. The expressions are given as follows:

$$C_{Howe} = \frac{2\pi\varepsilon_o l}{\ln\left(\frac{4}{D}\right) - 1} \quad , \quad D \ll 1 \tag{26}$$

$$C_{Butler} = \frac{2\pi^2\varepsilon_o d}{\ln(16D)} \quad , \quad D \gg 1 . \tag{27}$$

Butler [21] observed that the parameter range for each expression can be relaxed without serious error. He noted that at $D \cong 0.25$ both expressions produce results within 4% of the precise value obtained by the method of moments, thereby allowing one the means of computing the capacitance by using the appropriate expression above or below $D \cong 0.25$.

Figure 11 shows the regions of acceptable accuracy of the tubular monopole capacitance formulas and the free space tubular capacitance formulas. Some of the fine detail has been removed for clarity. The extended Grover formula (17) is omitted since its useful region is close to that of Grover. Note that the Grover formula overlaps with that of Howe while the CMA result approaches the approximate free space boundary in an asymptotic fashion.

7. APPLICATION TO A TUBE OF NONCIRCULAR CROSS SECTION

The concept of modeling an antenna of noncircular cross section with one of circular cross section having an effective radius that yields the same input impedance and radiation pattern was first introduced by Hallén [22]. This concept applies to electrically small antennas. If the capacitance of the feed region is negligible, the effective radius for a monopole of noncircular cross section can be computed with the aid of expressions from several sources [23-25] and used in the capacitance expressions given in this report. However, it must be emphasized that these results are approximate.

8. SUMMARY

Formulas have been presented for the computation of the input capacitance of electrically small tubular monopoles for a wide range of diameters and heights above ground. The regions of validity for the existing formulas were determined through comparison with precise results obtained from a standard method of moments code. Several regions lying between the thin and thick tube domains were identified where the existing formulas are not applicable. As a result, an approximate expression was constructed, effectively bridging the gap between the thin and thick tube domains. Taken as a whole, such an assembly of formulas allows for the determination of capacitance for a continuous range in terms of the normalized variables D and H for over six orders of magnitude, with errors usually much less than 10%. For large ground plane separations, it was shown that the monopole formulas approach the results obtained for a tube in free space.

For information on various relevant topics including capacitance formulas for several tubular monopole feeds and the numerical convergence of the method of moments algorithm used in this investigation, the reader is referred to the appendices.
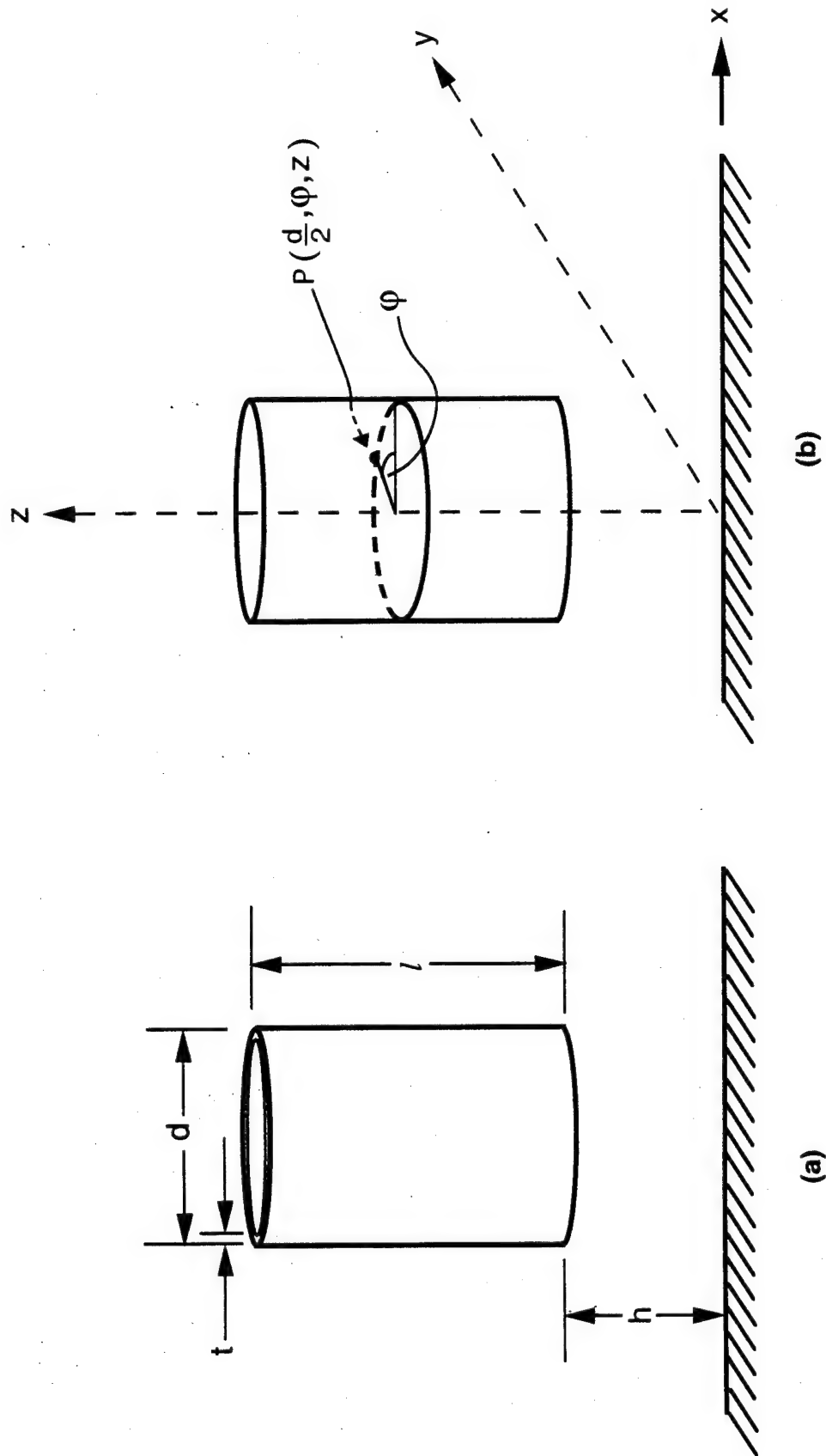
Figure 1. (a) Tubular monopole.
(b) Coordinate system used for tubular monopole analysis.
Note: t « d, *l*.
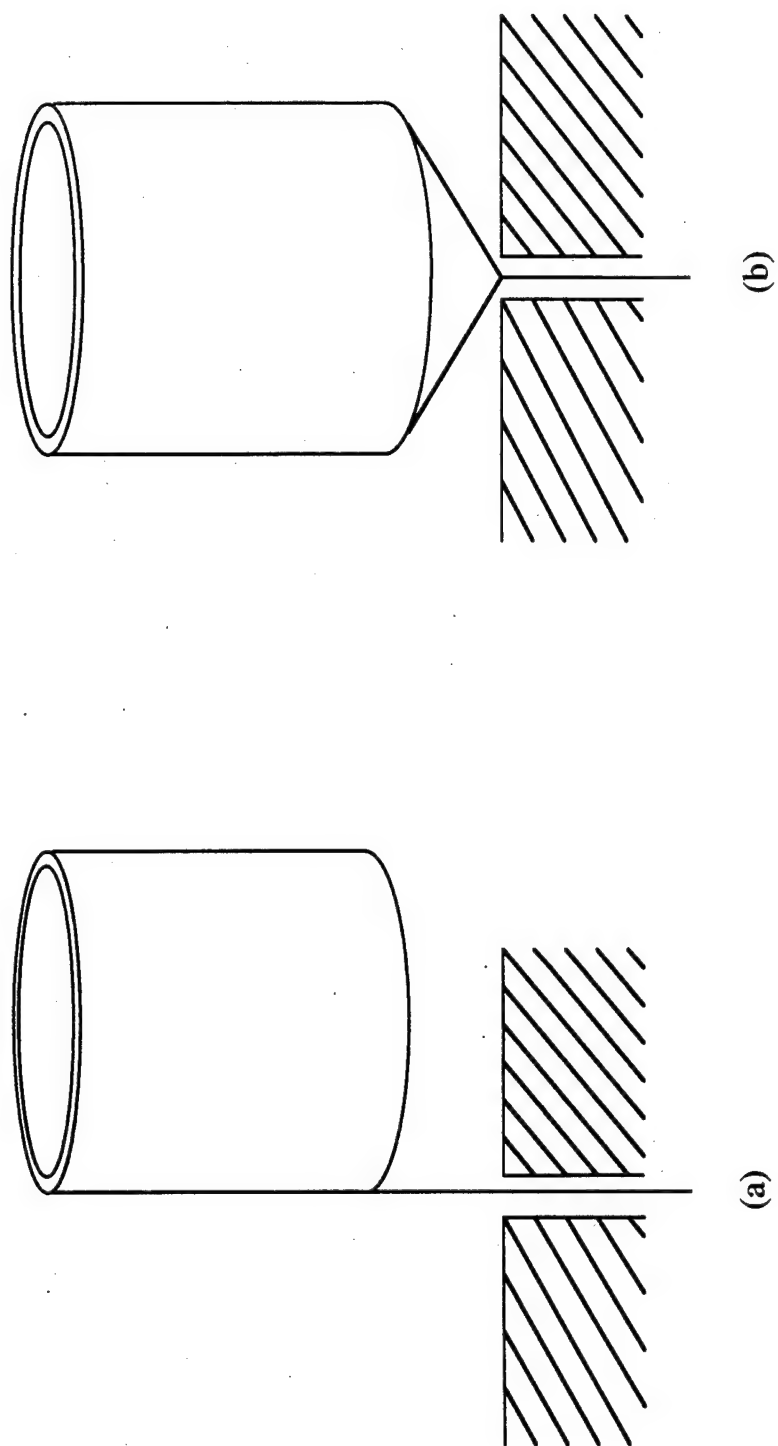
Figure 2. Typical methods for feeding tubular monopoles.
(a) Wire feed.
(b) Conical feed.

$$\frac{q(z)}{\varepsilon_o V}$$
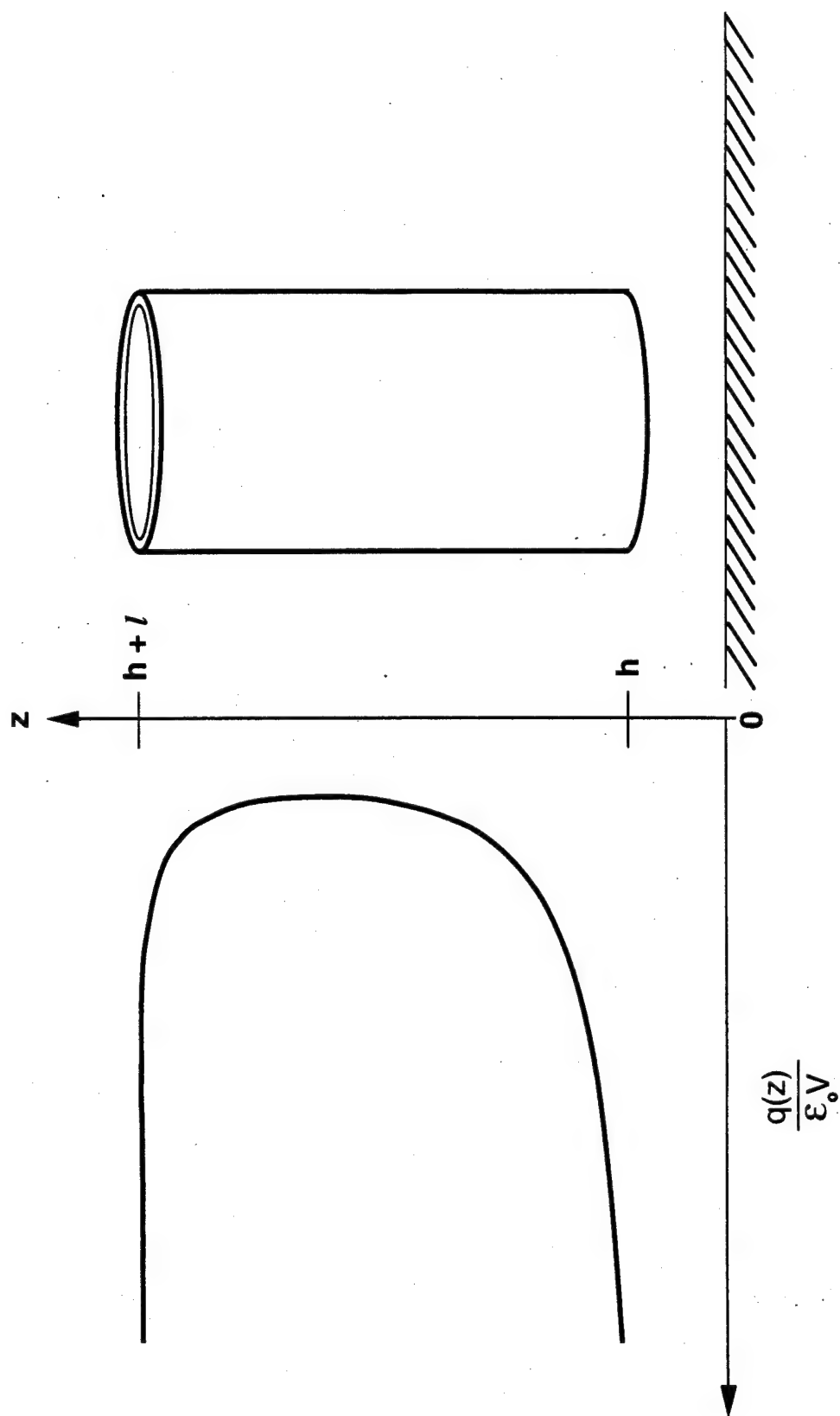
Figure 3.   Charge distribution along a tubular monopole.
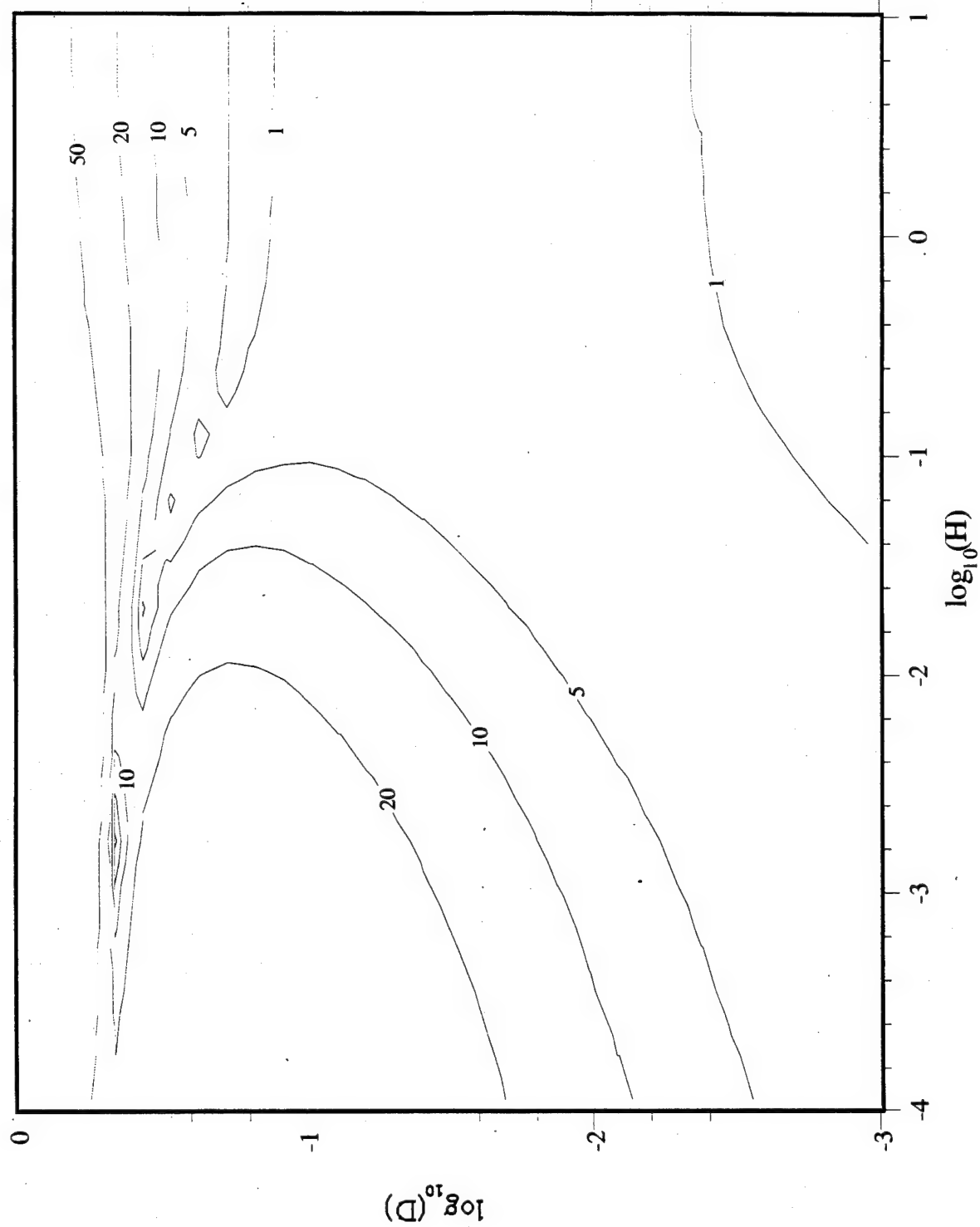
Figure 4. Error contours for Grover's formula (6).
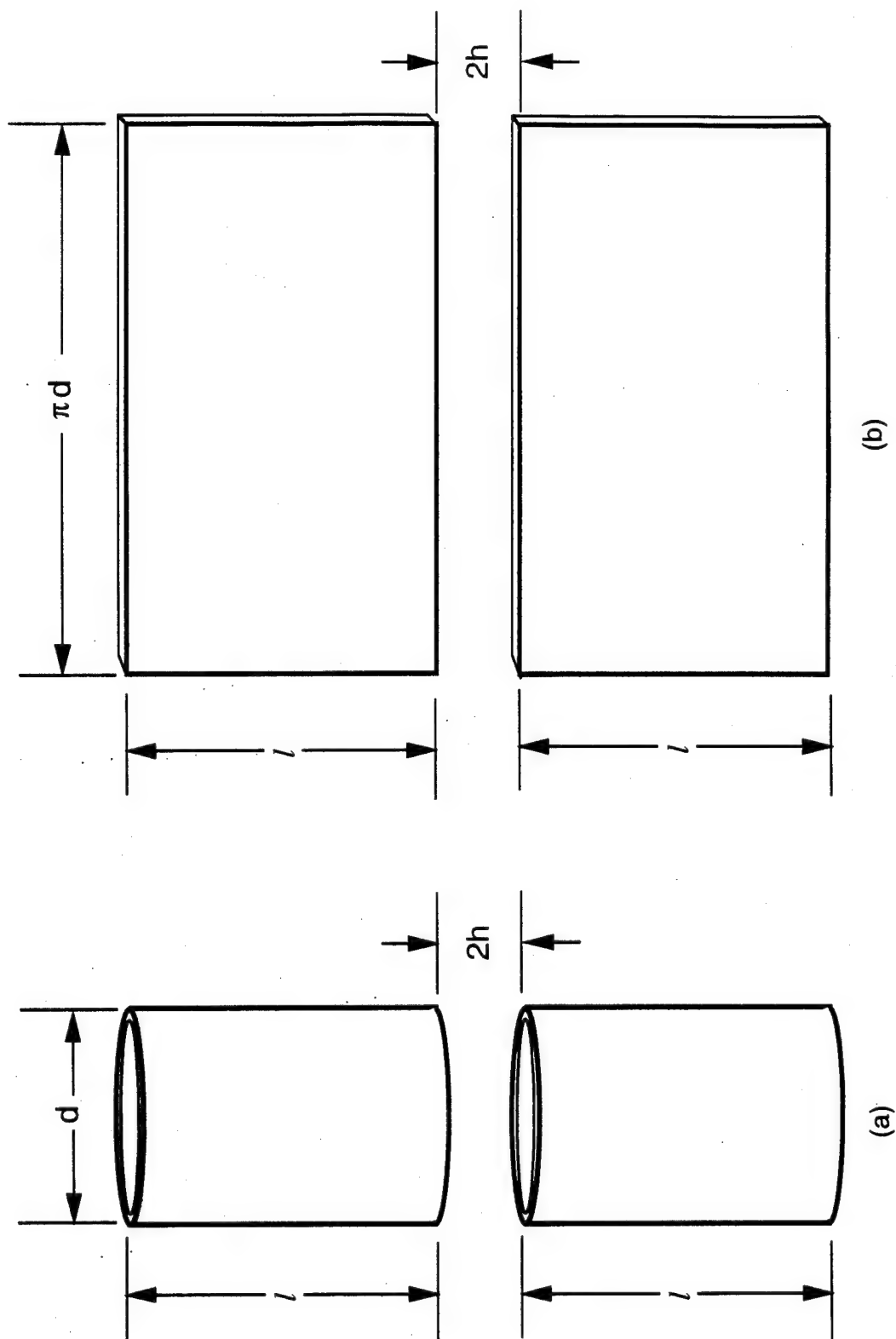
Figure 5 Model used in the derivation of the conformal mapping approximation (8).
(a) Tubular dipole.
(b) Equivalent coplanar stripline.
Note: tube thickness is assumed to be infinitesimal.
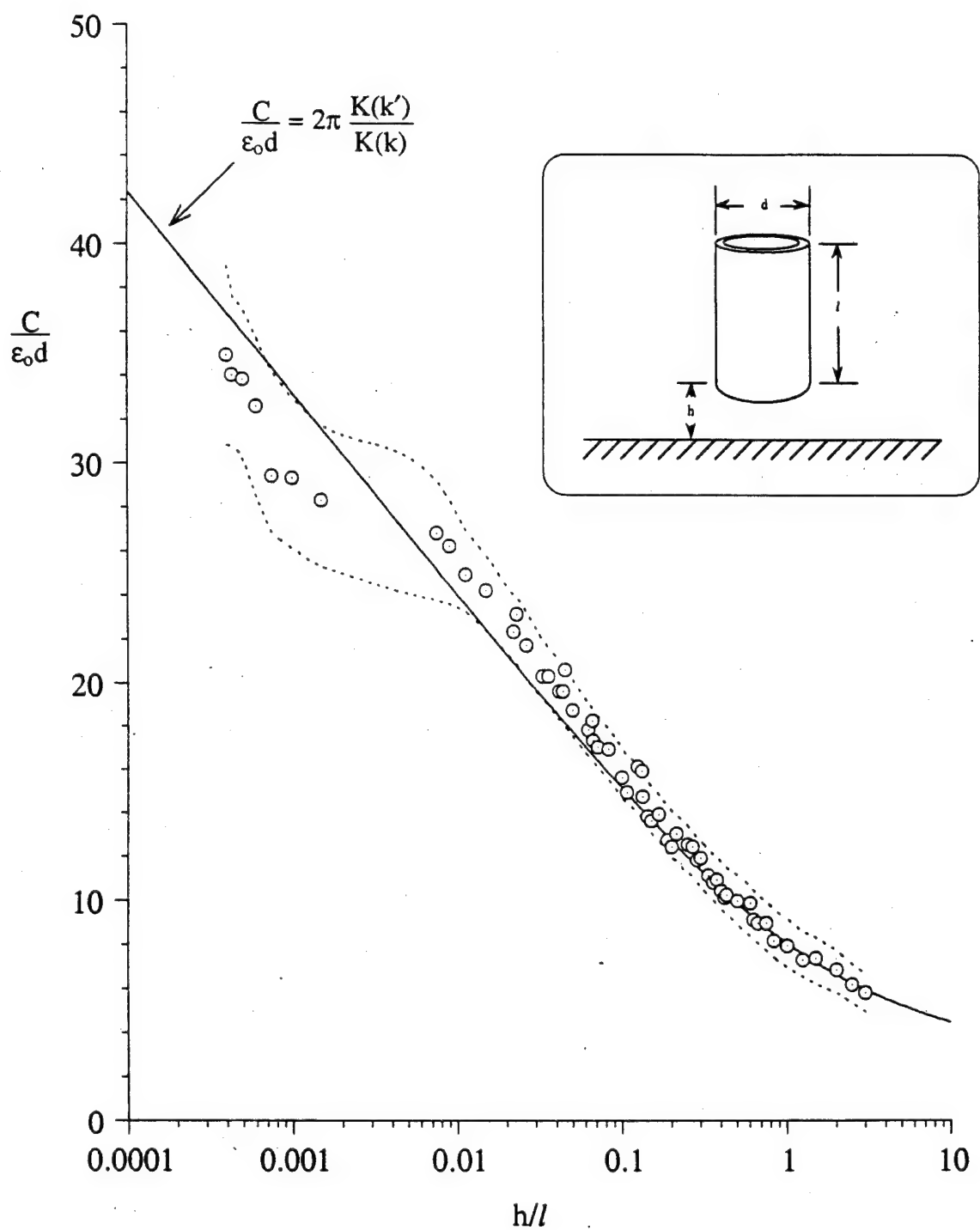
Figure 6. Comparison of normalized capacitance using CMA formula (8) and measured data. The dashed lines are the error bounds in the measurements.
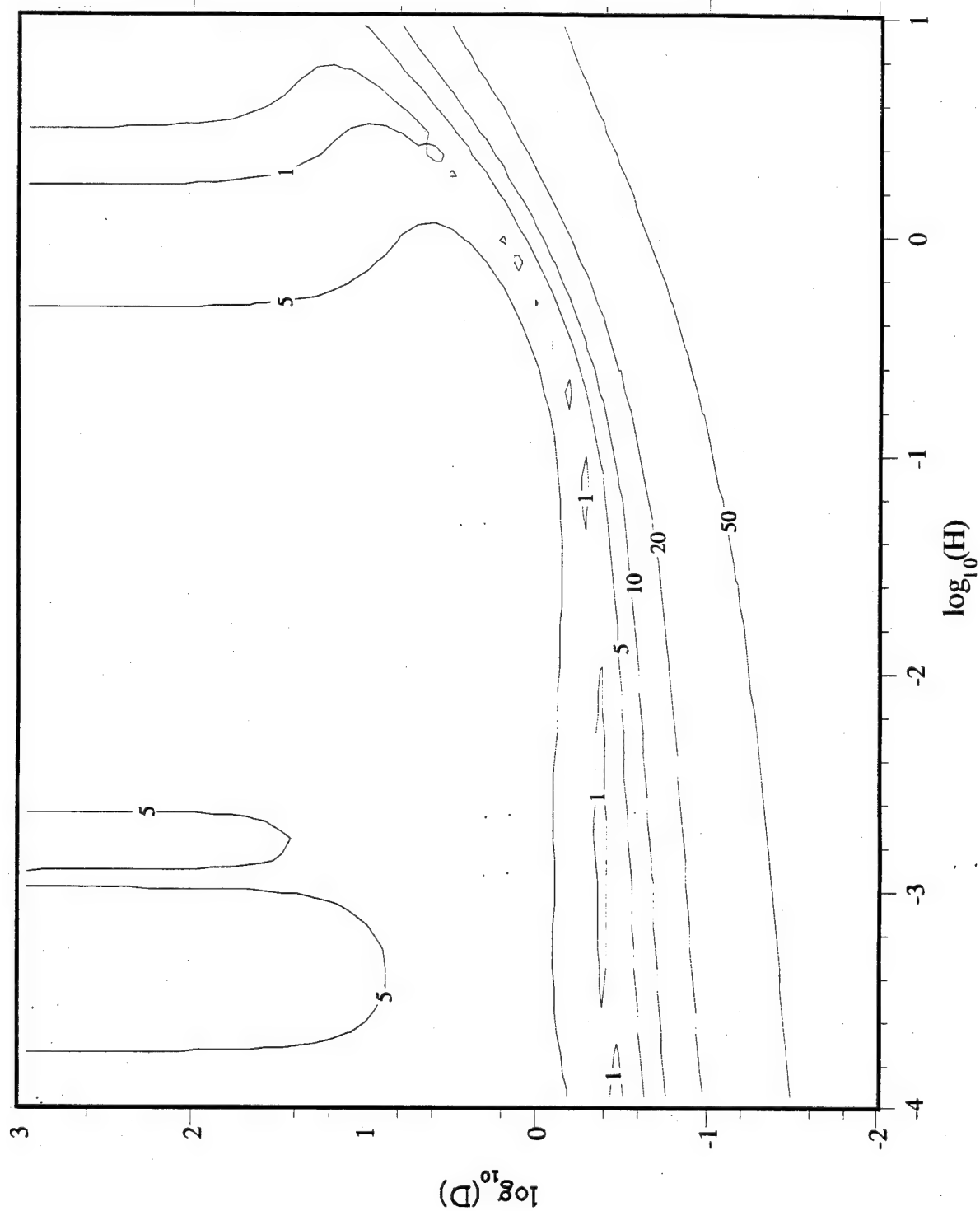
Figure 7. Error contours for the conformal mapping approximation (8).
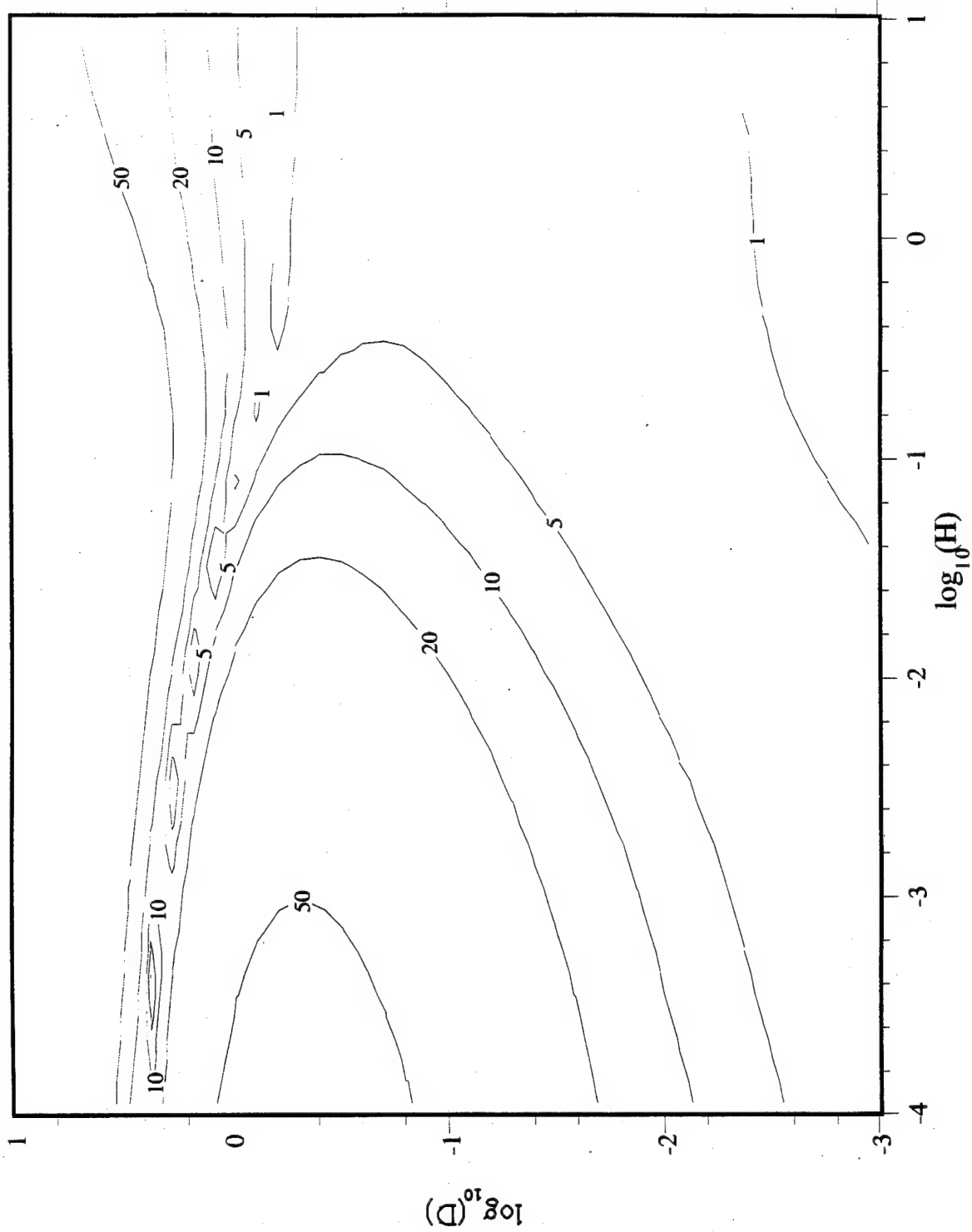
Figure 8.   Error contours for the extended Grover formula (17).
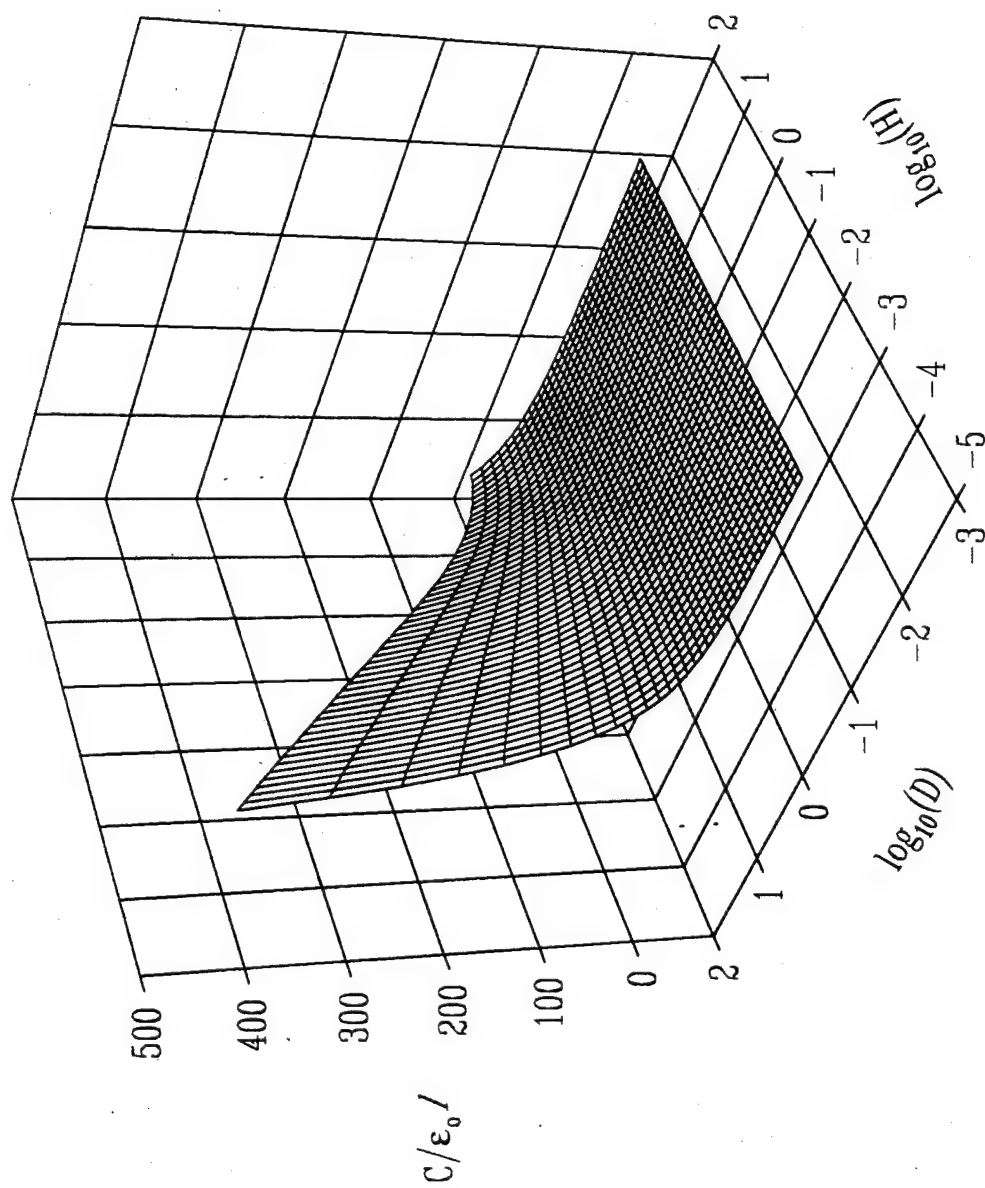
Figure 9. Surface of the normalized tubular monopole capacitance used to determine ACF (23).
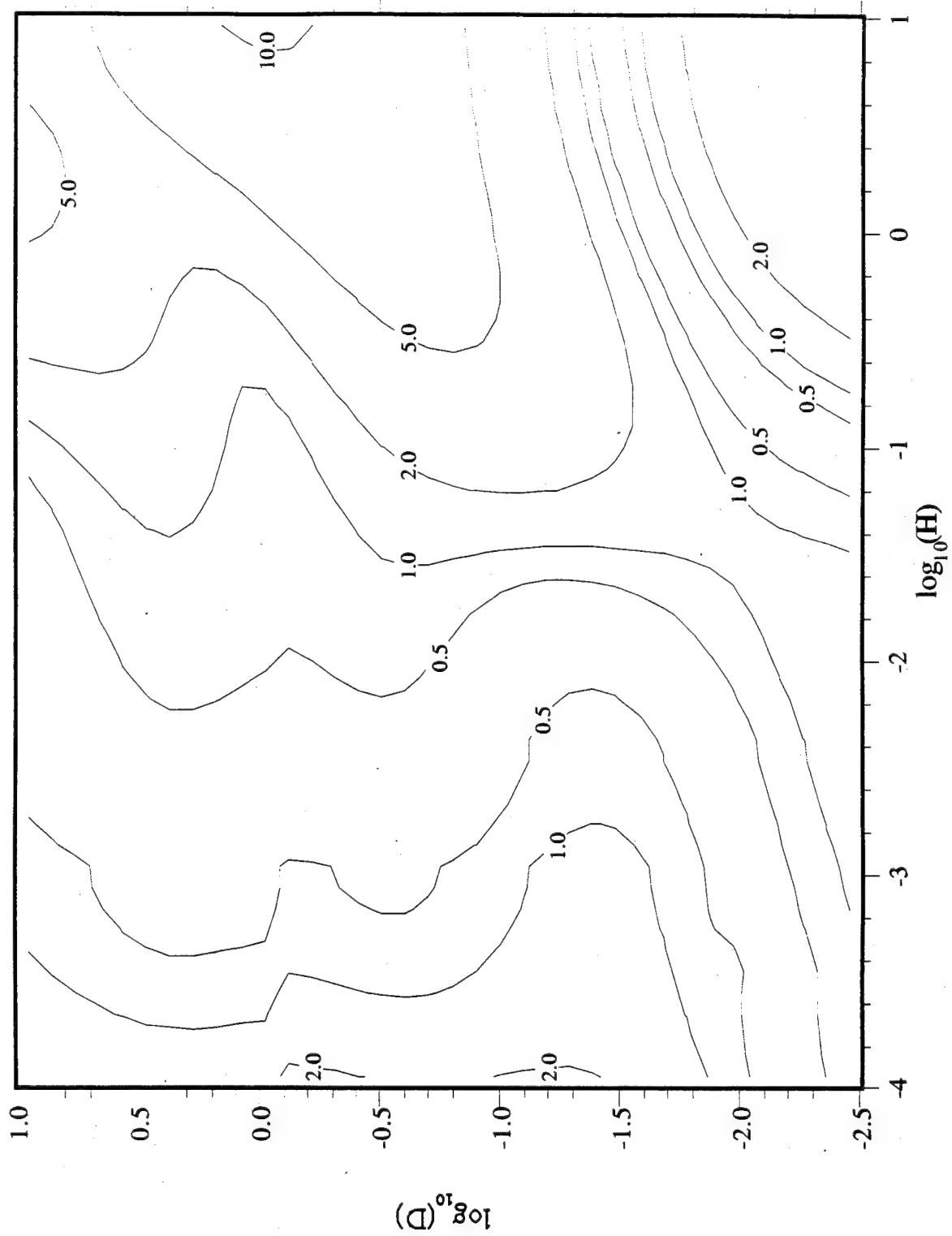
Figure 10. Error contours for the approximate capacitance formula (23).
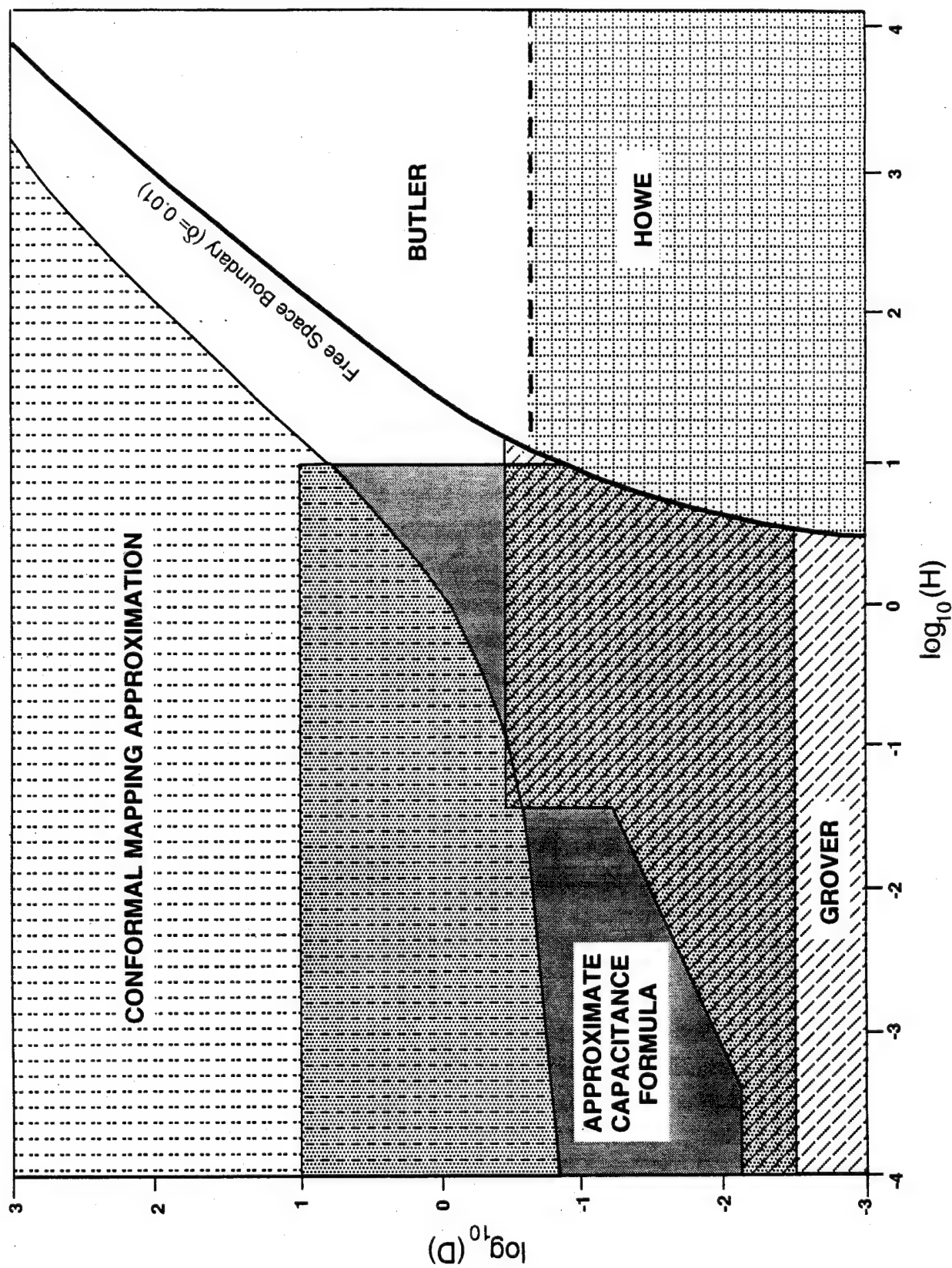
Figure 11   Regions of validity (error ≤ 10%) of tubular monopole capacitance formulas
Note: $H = h/l$, $D = d/l$.

Table I. Ranges of Validity of Tubular Capacitance Formulas
(Error ≤ 10%)

Formula	Range of H (H = h / l)	Range of D (D = d / l)
Grover (6)	≤ 0.0004	≤ 0.008
	$0.0004 \leq H \leq 0.04$	$\leq 0.27\,H^{\,0.45}$
	≥ 0.04	≤ 0.35
Extended Grover (17)	≤ 0.0005	≤ 0.007
	$0.0005 \leq H \leq 0.1$	$\leq 0.33\,\sqrt{H}$
	≥ 0.1	≤ 1
Approximate Capacitance Formula (ACF) (23)	$10^{-4} \leq H \leq 10$	$0.003 \leq D \leq 10$
Conformal Mapping Approximation (CMA) (8)	$\geq 10^{-4}$	$\geq \dfrac{2}{\ln\left(1 + \dfrac{3}{H}\right)}$

APPENDIX A

CAPACITANCE FORMULAS FOR TUBULAR MONOPOLE FEEDS AND OTHER EFFECTS

1. Introduction

In this report, the monopole was considered as a charged vertical tube above a ground plane. The tube was considered to have an infinitesimally thin wall and no connecting wires. In actual practice, a monopole antenna has some finite wall thickness, however small, and is fed in a definitive fashion. The total input capacitance of a practical antenna must therefore account for such effects. In this appendix, some capacitance expressions for these effects, suitable for practical antenna analysis and design, are summarized.

2. Summary of capacitance formulas

2.1. Correction for finite wall thickness

A correction to account for the finite thickness of the tubular monopole is developed by solving the analogous problem of the excess (or incremental) capacitance-per-unit length of two oppositely charged coplanar plates of thickness t and separation s, as shown in Fig. A-1(a). The correction ΔC is here defined as the difference of the per-unit-length capacitance $C(t, s)$ of the coplanar plate structure with finitely thick plates and the per-unit-length capacitance $C(0, s)$ of the same structure with plates having zero thickness :

$$\Delta C = C(t, s) - C(0, s) \quad . \quad . \tag{A-1}$$

This result is then rearranged to yield the desired correction for the case of a charged vertical plate whose edge is parallel and over a ground plane, as shown in Fig. A-1(b).

The plates in Fig. A-1(a) extend to infinity in both directions of the vertical plane and the correction is computed in the direction normal to the page. The quantities $C(t, s)$ and $C(0, s)$ are determined through conformal mapping. When combined with (A-1), an implicit solution results and is given by Cohn [26] as

$$\Delta C = \frac{2}{\pi} \varepsilon_0 \ln\left[\frac{2\, E(k) - k'^2\, K(k)}{2\, \sqrt{k}} \right] \;, \tag{A-2a}$$

where k is related to t/s by

$$\frac{t}{s} = \frac{(1+k^2)\,K(k') - 2\,E(k')}{2\left[2\,E(k) - k'^{\,2}\,K(k)\right]} \quad , \tag{A-2b}$$

and

$$k' = \sqrt{1 - k^2} \quad . \tag{A-2c}$$

In (A-2), $K(k)$ and $E(k)$ are the complete elliptic integrals of the first and second kinds, respectively [19]. A plot of ΔC as a function of t/s can be obtained by evaluating (A-2a) and (A-2b) individually, by varying the modulus k from zero to one. A plot constructed in this way is shown in Fig. A-2. In the plot, the value of the difference $[\Delta C - (\varepsilon_o t/s)]/\varepsilon_o$ as a function of t/s was obtained by varying k from 0.001 to 0.999, in increments of 0.001. The second term of the difference, $(\varepsilon_o t/s)$, is the capacitance-per-unit-length of the gap region shown in Fig. A-1, neglecting fringing effects.

An inspection of Fig. A-2 shows that for $t/s \geq 1$, $[\Delta C - (\varepsilon_o t/s)]/\varepsilon_o$ approaches a constant and is negligible for $t/s \leq 0.001$. A good approximation for (A-2) that eliminates the intermediate computations involving k and is applicable for all values of $t/s \geq 0.001$, has the following form:

$$\frac{\Delta C}{\varepsilon_o} \cong \left(\frac{t}{s}\right) + \frac{1}{24\sqrt[3]{1 + \left[\frac{1}{6\left(\frac{t}{s}\right)}\right]^2}} \quad . \tag{A-3}$$

Expression (A-3) is accurate to three significant figures. Referring again to Fig. A-1(b), the corresponding thickness correction for the vertical plate above a ground plane is obtained by substituting $2h = s$ into (3), followed by a doubling of the right hand side of the expression. The correction for the unsymmetrical case thus becomes

$$\frac{\Delta C}{\varepsilon_o} \cong \left(\frac{t}{h}\right) + \frac{1}{12\sqrt[3]{1 + \left[\frac{1}{3\left(\frac{t}{h}\right)}\right]^2}} \quad . \tag{A-4}$$

Expression (A-4) is accurate to three significant figures for $t/h \geq 0.001$. The expression is general enough so that it can be applied to a tubular monopole of arbitrary cross section when multiplied by the *mean* perimeter of the tube. As an example, the thickness correction for a tubular monopole with a circular cross section is obtained by multiplying the per-unit length correction (A-4) by the mean circumference P_{mean} of the tube, i.e.,

$$P_{mean} = \pi\,(a + b) \quad ,$$

where a and b are the inner and outer radii of the tube, respectively. Upon substitution of P_{mean}

into (A-4), the correction is given as

$$\Delta C \cong \pi \, \varepsilon_0 \, (a + b) \left\{ \left(\frac{t}{h} \right) + \frac{1}{12 \sqrt[3]{1 + \left[\frac{1}{3 \left(\frac{t}{h} \right)} \right]^2}} \right\} \; . \qquad \text{(A-5)}$$

The capacitance correction given by (A-5) is added to the capacitance computed for a thin walled cylinder. In the application of an appropriate thin-wall capacitance expression to a tube of arbitrary cross section and wall thickness, it is suggested that the *mean effective* diameter be used.

The range of validity of (A-2) is given by Cohn [26] as:

$$\frac{s}{\lambda} \leq \frac{1}{4} \quad \text{and} \quad \frac{s}{r} \leq \frac{1}{2} \; ,$$

where s is the gap distance between the plates [see Fig. A-1 (a)] and r is the distance from the center point of the configuration to the nearest *extraneous surface*. An example of an extraneous surface is shown in Fig. A-3 for the case of a capacitive iris in a waveguide. In this figure, the distance r is measured from the center line of the capacitive iris to the adjoining waveguide walls. The range of validity for the corresponding case of the tubular monopole is found by setting 2h = s and r = h+l and substituting them into the above inequalities. The use of r = h+l is made because an extraneous surface (in the form of a top load) may be placed at this distance to increase the effective height of the antenna. The ranges of validity for the corresponding tubular monopole case are then

$$\frac{h}{\lambda} \leq \frac{1}{8} \quad \text{and} \quad \frac{h}{l} \leq \frac{1}{3} \; .$$

In the present application, the monopole is electrically small so that h+l ≤ λ/8, thereby satisfying the first inequality. The second inequality is satisfied in most practical designs.

2.2. Thin wire feed capacitance

The geometry of a thin wire used to feed a tubular monopole is shown in Fig. A-4. As shown in the figure, the wire is a continuation of the center conductor of a coaxial cable and is attached to the lower end of the tube. The capacitance of the feed wire is given by King [16] as

$$C_{feed} \cong \frac{2\pi\varepsilon_0 h}{\ln\left(\frac{2h}{a}\right) - 1} \left[1 + \frac{\ln 2}{\ln\left(\frac{2h}{a}\right) - 1} \right] \; , \qquad \text{(A-6)}$$

where h and a are the height and radius of the feed wire, respectively. Expression (A-6) is valid

27

for $h/a \geq 75$ and $h \leq \lambda/8$.

2.3. End correction for a coaxial line

In conventional transmission line theory, for a given cross section, it is assumed that the charge-per-unit-length on each conductor is equal in magnitude but opposite in sign. The capacitance per-unit-length derived under this assumption becomes a function of only the cross section. However, if the same line is connected to an antenna, the charge distribution in the region of transition undergoes a change. This has the effect of altering the antenna admittance measured at some distance from the antenna, compared with the admittance predicted using standard transmission line expressions.

Figure A-5 provides a view of the transition from a coaxial cable to a thin monopole antenna. The portion of the transmission line along which the charge distribution differs from that usually assumed, will be referred to as the transition region. The transition region extends from $w = 0$ to $w = d$, where w is defined in Fig. A-5. The measured apparent admittance Y_a of a monopole antenna is given approximately by King [27] as

$$Y_a \cong Y_o + j \omega C_T \ , \quad \text{for} \ b/a > 1 \ , \tag{A-7}$$

where

$$C_T = \int_0^d \left[\, c(w) - c_o \,\right] dw \ . \tag{A-8}$$

In (A-7), Y_o is the ideal theoretical admittance, C_T is the lumped equivalent transition capacitance, that is placed at $w=0$ (see Fig. A-5) to account for the disturbance in charge distribution in the transition region of the transmission line. The per-unit-length capacitances $c(w)$ and c_o in (A-8) are for the transition region and coaxial line, respectively. Note that $Y_a \rightarrow Y_o$ as $b/a \rightarrow 1$. In (A-8), d is the range over which the difference $c(w) - c_o$ is significant, extending to $d \cong 10b$. It is seen from (A-7) that the determination of the lumped transition capacitance C_T, which has a *negative* value, is important in order to accurately quantify the antenna's input admittance.

King [27] theoretically determined the normalized transition capacitance, $- C_T/c_o b$, in the limits of large and small outer-inner conductor ratios b/a. A plot of the approximate computation, along with an extrapolated curve joining the two regions (derived by King), is shown in Fig. A-6. Included in this figure are some measured data obtained by Hartig [28]. From the figure, it can be seen that the measured values display the same general trend as the theoretical ones but are larger for $b/a \geq 2$. Because of the approximate nature of the theory used to predict the lumped transition capacitance, and the discrepancy in the scaling of Hartig's measurement values, King suggests

that either curve may be used to determine - $C_T/c_o b$.

In the absence of theoretical or measured data, a useful approximation for C_T that yields values intermediate between those of King and Hartig has the form

$$C_T \cong - 2\pi\varepsilon b \left[\frac{\ln(b/a)}{3+\ln^3(b/a)} \right] , \quad 2 \leq b/a \leq 30 . \tag{A-9}$$

Table A-1 is a chart comparing (A-9) against both theoretical and measured values.

2.4. Capacitance of a conical feed

Aside from the thin wire feed, another common way of feeding a monopole uses a cone, as shown in Fig. A-7. The classical method of determining the capacitance-per-unit length of an *infinite* cone above a ground plane has been derived by Schelkunoff [29] as:

$$C = \frac{2\pi\varepsilon_o}{\ln\left[\cot\left(\frac{\theta_o}{2}\right) \right]} . \tag{A-10}$$

The complicated nature of the boundary conditions on the edges of the truncated region prohibits an analytical treatment of the problem; recourse to numerical techniques becomes a practical alternative. Toward this end, Wilton [17] determined the capacitance of finite-length cones with and without a topcap above a ground plane using the method of moments for $2.5° \leq \theta_o \leq 87.5°$.

The capacitance data from Wilton's study was used to obtain an approximate expression for the capacitance of a conical feed. In deriving the approximate expression, an approach was taken whereby the normalized capacitances of the infinite cone (C/ε_o) and truncated cone ($C/\varepsilon_o L$) were plotted against the infinite cone half angle θ_o, to observe the deviation between the two cases. While some deviation in the capacitance curves for the two cases was noted, the curves were observed to be very similar in shape, suggesting that the functional dependence given by (A-10) was applicable. The deviation in capacitance between the two cases was consequently corrected by the substitution of an *effective* infinite cone half-angle θ_o^{eff} in place of the original cone half-angle θ_o in (A-10). The approximate expression for the capacitance of a truncated cone was thus derived with the following form:

$$C \cong \frac{2\pi\varepsilon_o L}{\ln\left[\cot\left(\frac{\theta_o^{eff}}{2}\right) \right]} , \tag{A-11}$$

where

$$\theta_o^{eff} = \theta_o \left[1 + \left(\frac{90^\circ - \theta_o}{\kappa} \right)^2 \right] , \text{ (deg.)}$$

and

$$\kappa = 74 \text{ (cone with a topcap)}$$
$$= 76 \text{ (cone without a topcap).}$$

The capacitances determined from (A-11) are within 6% of the method of moments data for $2.5^\circ \leq \theta_o \leq 87.5^\circ$.

2.5. Capacitance of an arbitrarily shaped plate above a groundplane

When the base of a short monopole has a plate attached to it, the plate capacitance along with the capacitance of the thin wire feed attached to the monopole must be known. A plate of arbitrary shape with surface area S and perimeter P situated above a ground plane, with an interposed dielectric of relative permittivity ε_r, is shown in Fig. A-8. Kuester [18, 30] has determined the capacitance of an arbitrarily shaped plate for the cases where either the narrowest dimension W_n is larger than the substrate height h or where the widest dimension W_w is smaller than the substrate height. The expressions (rearranged here for simplicity) are accurate within their regions of validity and are summarized below.

1. Narrowest plate dimension *larger* than the substrate height ($W_n / h > 0.5$):

$$C \cong \frac{\varepsilon_o \varepsilon_r S}{h} + \frac{\varepsilon_o P}{\pi} \left[1 + \ln \left(\frac{2P}{\pi h} \right) + A_1(P) + \varepsilon_r A_2(\varepsilon_r) \right] , \quad \text{(A-12)}$$

where

$$A_1(P) = \frac{1}{2P} \oiint_P \left[\frac{\overline{a}_n \cdot \overline{a'}_n}{\left| \overline{\rho}_o - \overline{\rho'}_o \right|} - \frac{(\pi / P)}{\left| \sin \frac{\pi (l - l')}{P} \right|} \right] dl \, dl' \quad \text{(A-13a)}$$

and

$$A_2(\varepsilon_r) \cong \frac{1}{2} \left(\frac{\varepsilon_r - 1}{\varepsilon_r} \right) \ln \left[1 - 0.6735 \left(\frac{\varepsilon_r - 1}{\varepsilon_r} \right) + 0.0788 \left(\frac{\varepsilon_r - 1}{\varepsilon_r} \right)^2 \right] + \ln (2\pi) . \quad \text{(A-13b)}$$

The variables used in the line integral $A_1(P)$ are illustrated in Fig. A-9 for an arbitrarily shaped plate. In addition, Table A-2 lists values of $A_1(P)$ for some common geometries.

2. Widest plate dimension *smaller* than the substrate height ($W_w / h < 0.5$):

$$C \cong \frac{2\pi\varepsilon_o(\varepsilon_r + 1)\, a_e}{\arctan\left[\dfrac{hB(\varepsilon_r)}{a_e}\right]} \quad , \tag{A-14}$$

where

$$B(\varepsilon_r) = \frac{\varepsilon_r - 1}{\varepsilon_r \ln\left(\dfrac{2\,\varepsilon_r}{\varepsilon_r + 1}\right)} \quad . \tag{A-15}$$

In (A-14), a_e is the effective radius of the plate. Various methods has been devised to compute a_e, with most of them numerical [10, 31-36]. Among the analytical methods, those of Pólya and Szegö [37] and Fabrikant [38] are simple. The method presented in [37] solves for the limits within which a_e exists, using lower and upper bound radii (a_l and a_u). In contrast, [38] utilizes an integral to estimate the effective radius, using the plate's centroid as the origin. The former method is easier to use because the area S and perimeter P of the plate are the only quantities required. In obtaining a close estimate of a_e using upper and lower bound radii, Kuester [18] has suggested taking the arithmetic-geometric mean (AGM) of the two quantities, given by

$$a_{e,\,AGM} = \frac{\pi\, a_u}{2\, K\left[\sqrt{1 - \left(\dfrac{a_l}{a_u}\right)^2}\right]} \quad , \tag{A-16}$$

where

$$a_l = \sqrt{\frac{S}{\pi}} \tag{A-17}$$

and

$$a_u = \frac{1}{2}\left[\frac{P}{2\pi} + \sqrt{\frac{S}{\pi}}\right] \quad . \tag{A-18}$$

In (A-16), $K[\cdot]$ is the complete elliptic integral of the first kind [19]. Effective radii for various plate shapes, taken from [18], are given in Table A-3. For plate shapes other than those listed in Table A-3, expressions (A-16) to (A-18) may be used to estimate a_e.
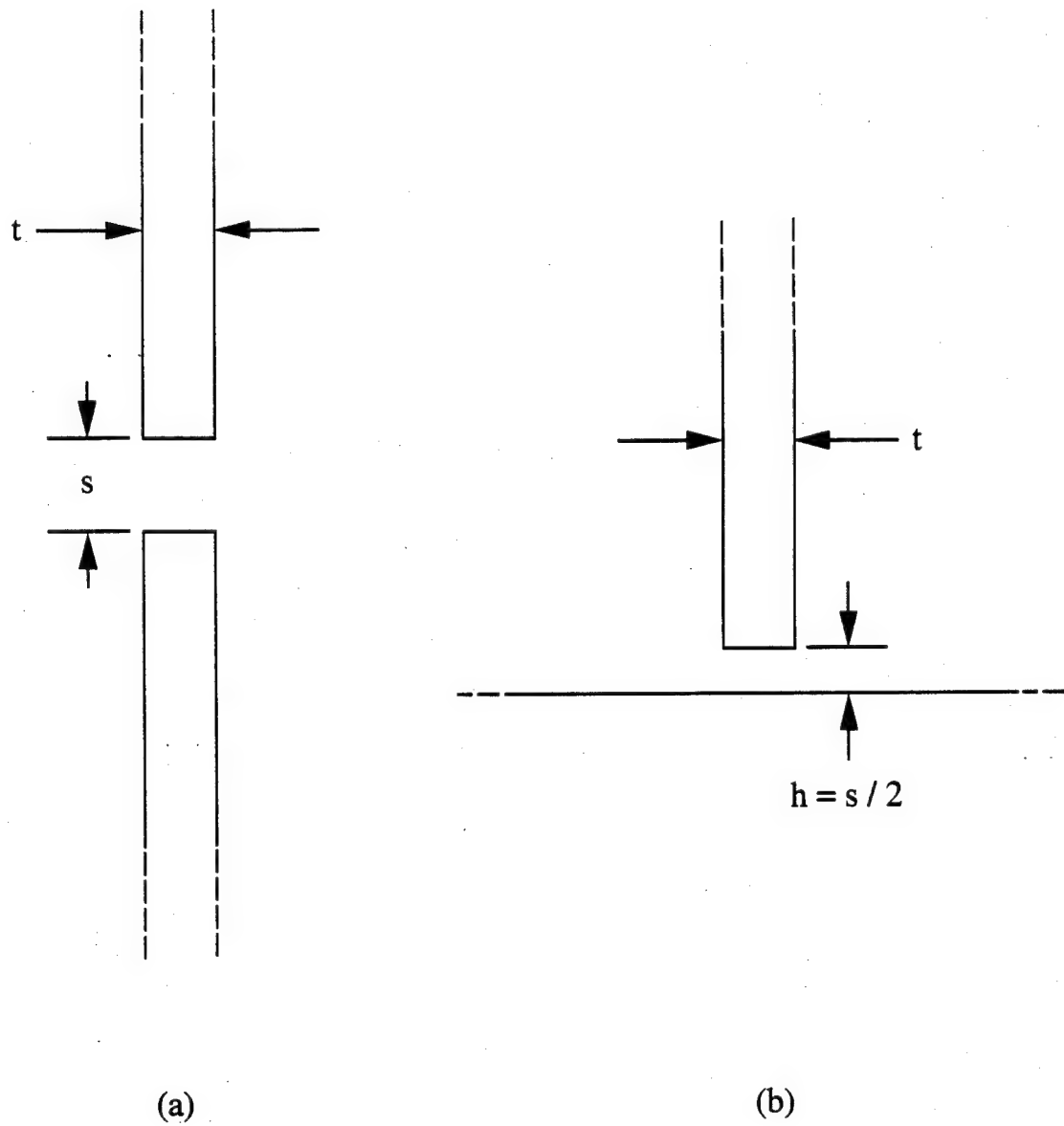
Figure A-1. Semi-infinite coplanar plate cross section.
(a) Symmetrical arrangement;
(b) unsymmetrical equivalent.
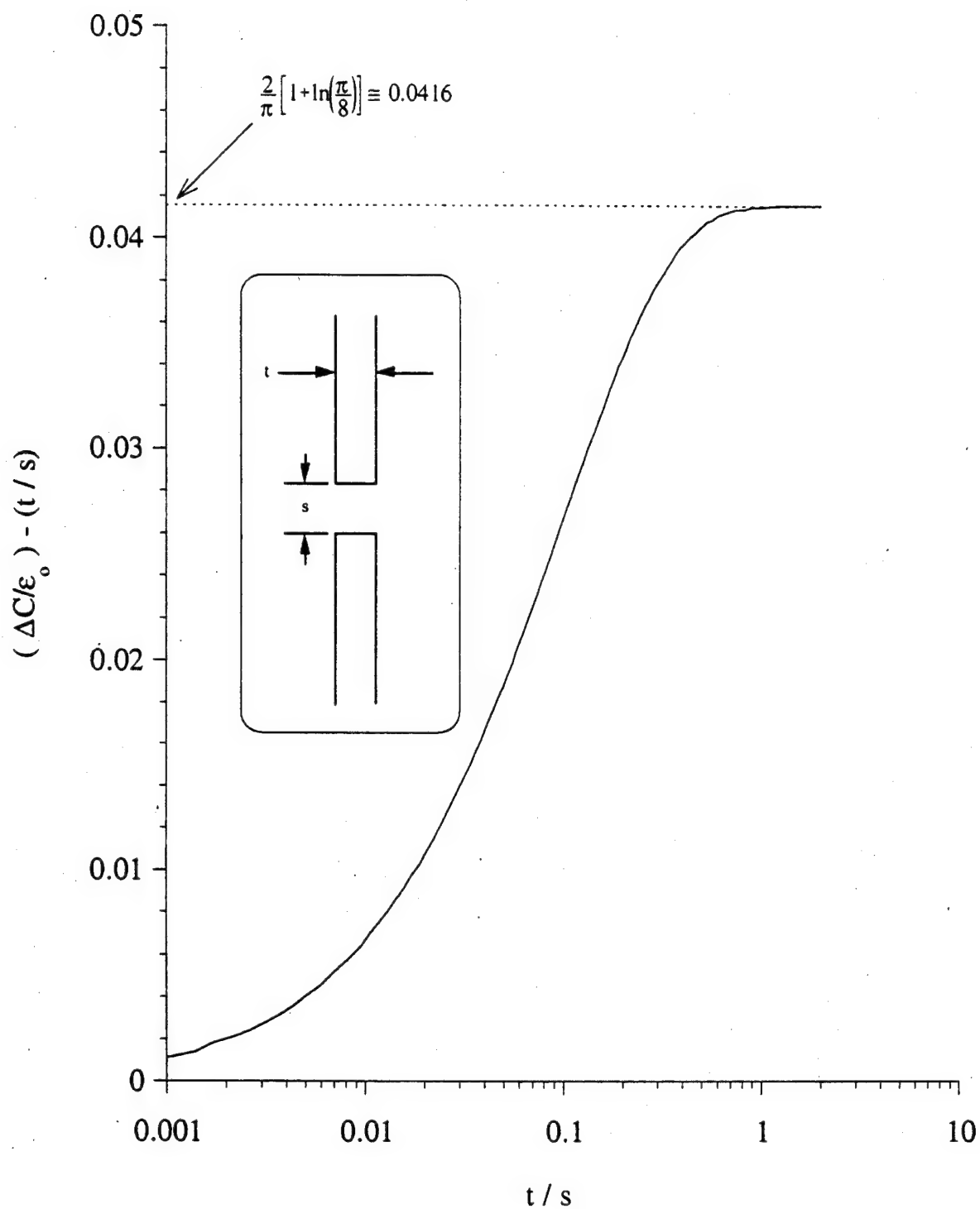
Figure A-2. Thickness correction for symmetrically arranged coplanar plates.
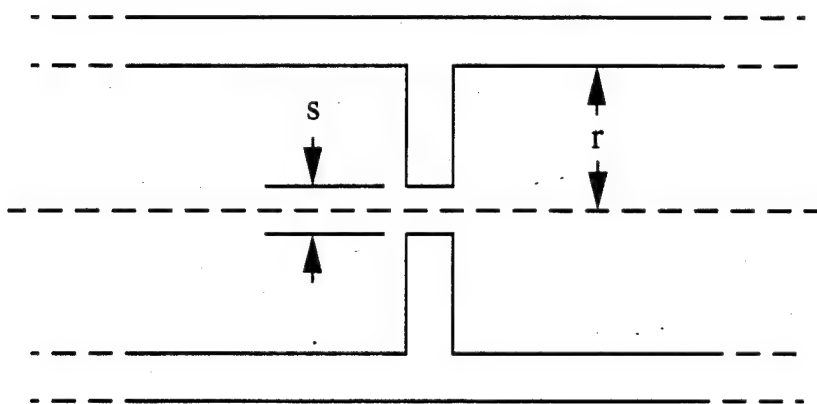
Figure A-3. Lengthwise view of a capacitive iris in a
waveguide. The nearest extraneous
surface in the illustration is the
waveguide wall. From Cohn [26].
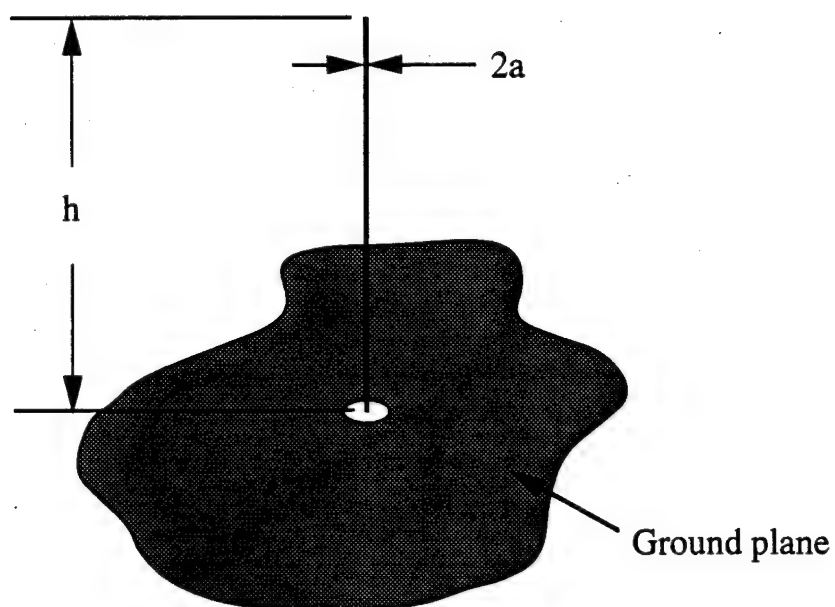
Figure A-4. Thin-wire feed configuration.

Thin feed wire / monopole

2a

Ground plane

w=0 (dashed line)

2b

w
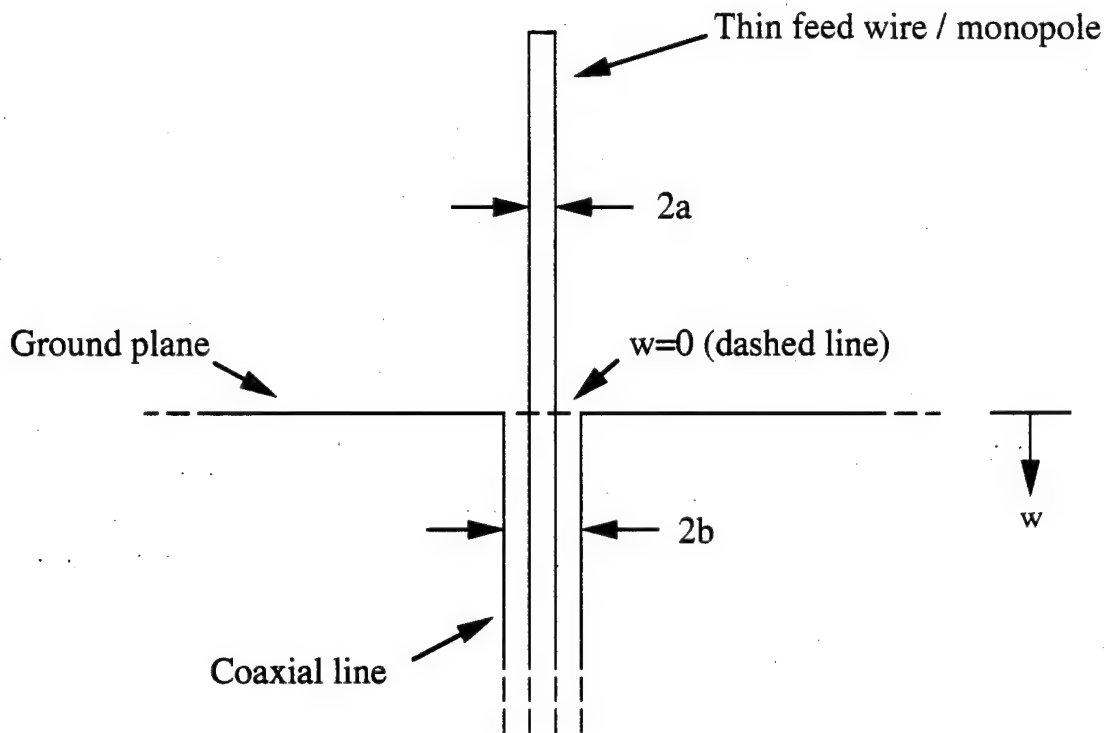
Coaxial line

Figure A-5. Cross section of coaxial line / monopole transition (w=0). The quantities 2a and 2b denote the inner and outer diameters, respectively.
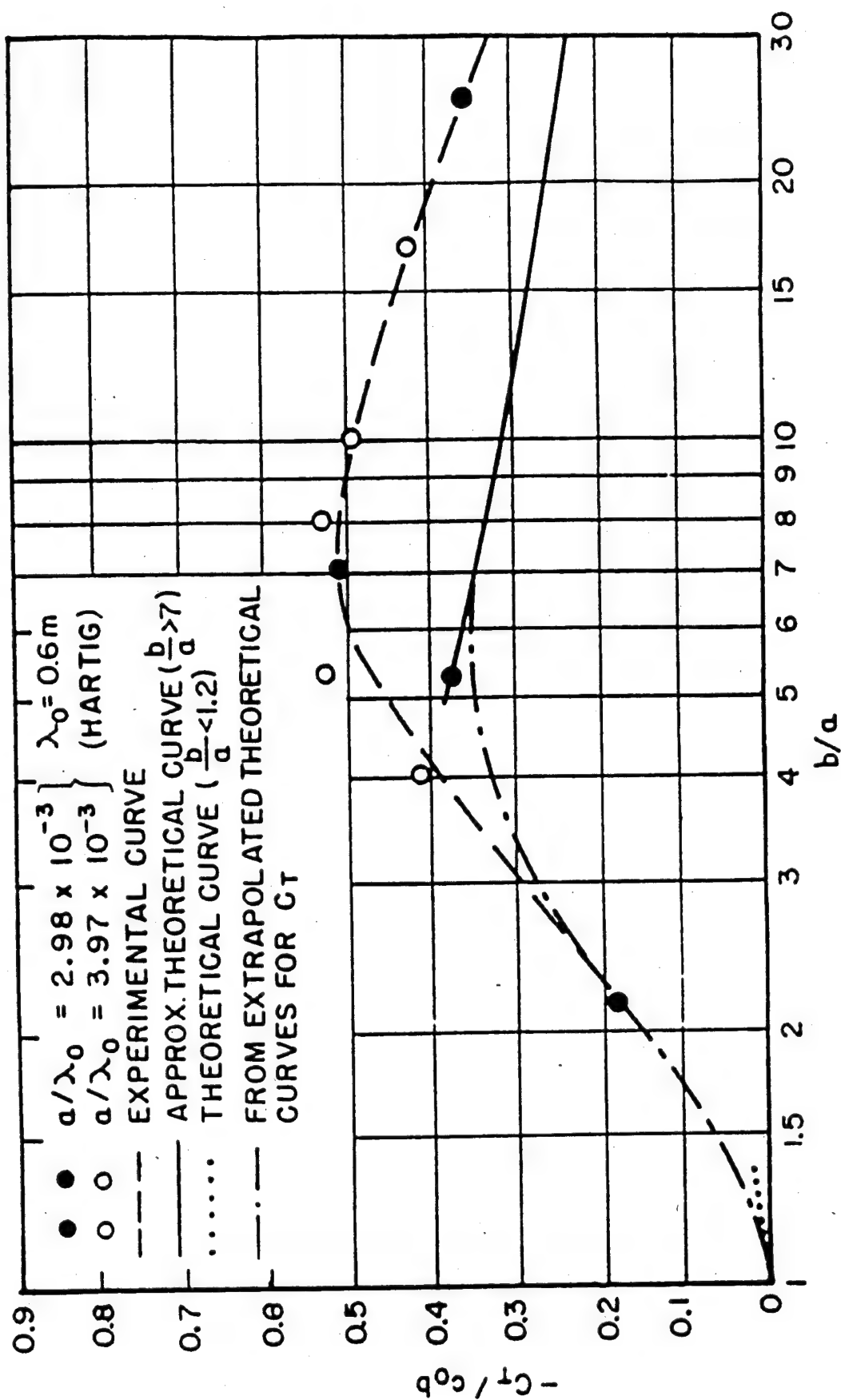
Figure A-6. The normalized transition capacitance for a monopole driven by a coaxial line. Figure from King [27].
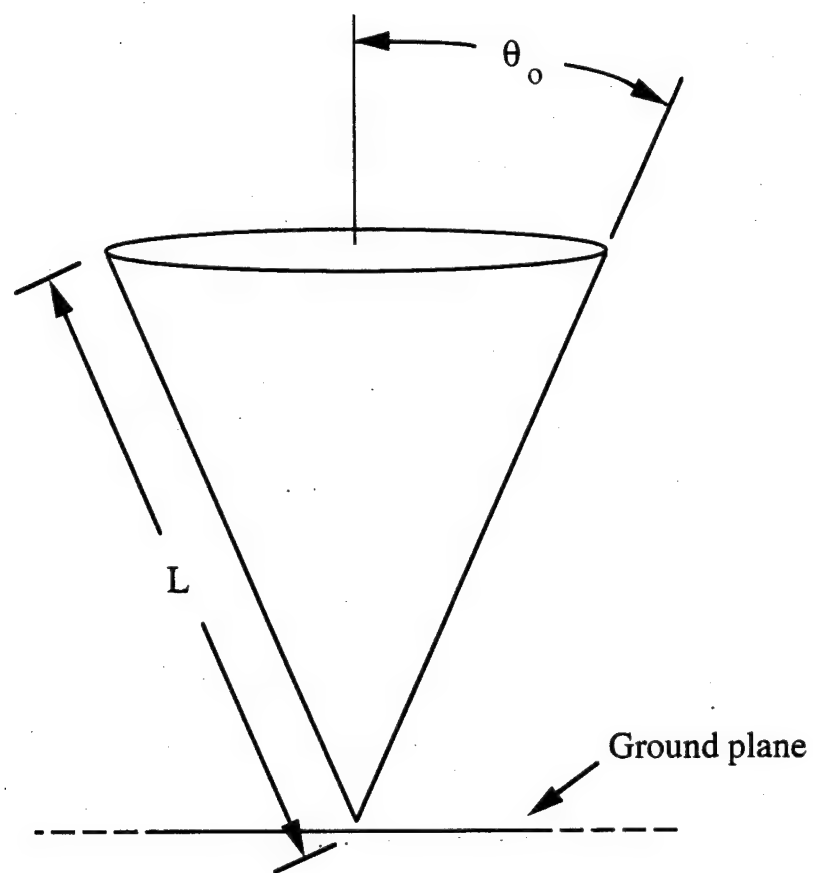
Figure A-7. Truncated cone with tip pointed toward the ground
plane. Tip is close to, but does not touch the ground
plane.

Surface area (S)

Perimeter (P)

Interposed dielectric

h
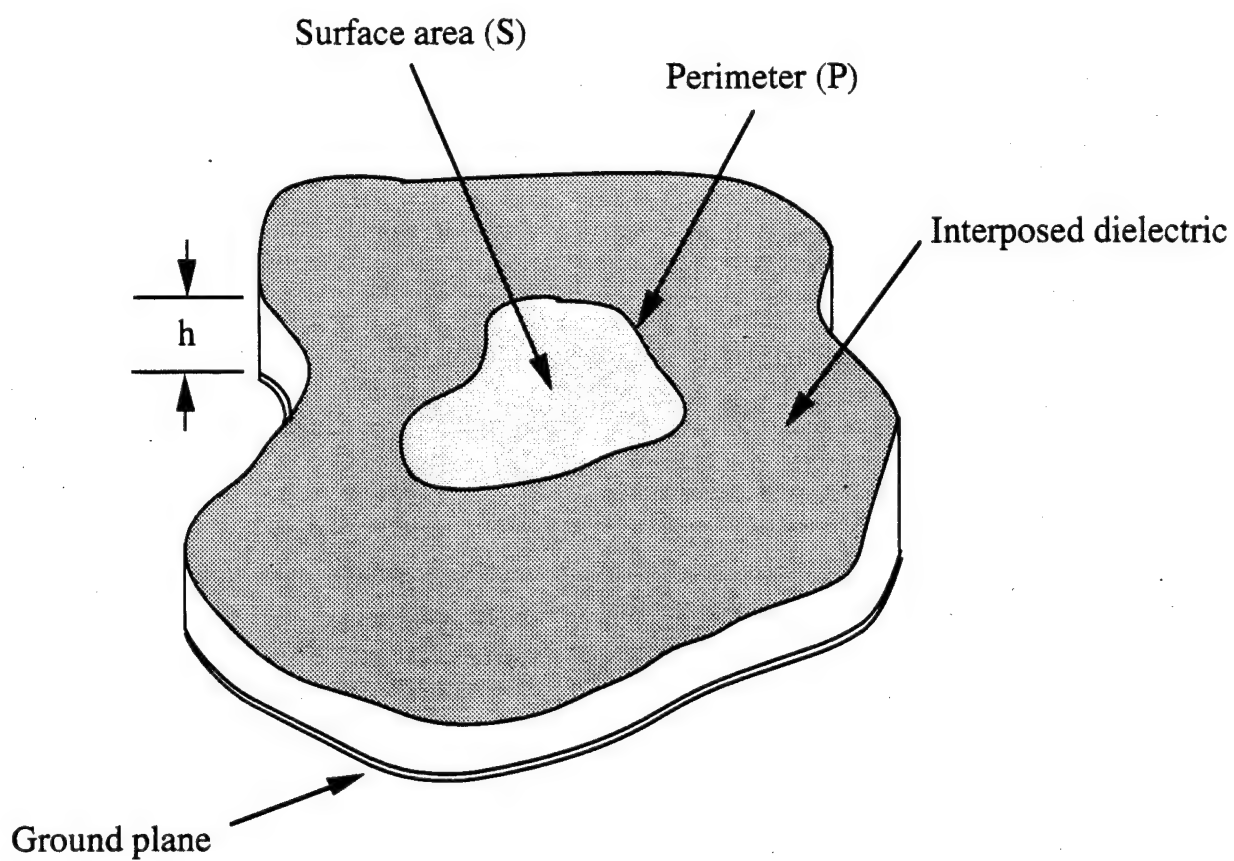
Ground plane

Figure A-8. Plate of arbitrary shape over a ground plane with interposed dielectric. Thickness (or height) of dielectric is h.

Perimeter (P)

$$\overline{dl}$$

$$\left| \overline{\rho_o} - \overline{\rho'_o} \right|$$

$$\overline{a_n}$$

$$\overline{a'_o}$$

$$\overline{dl'}$$

$$\overline{\rho'_o}$$

$$\overline{\rho_o}$$

O
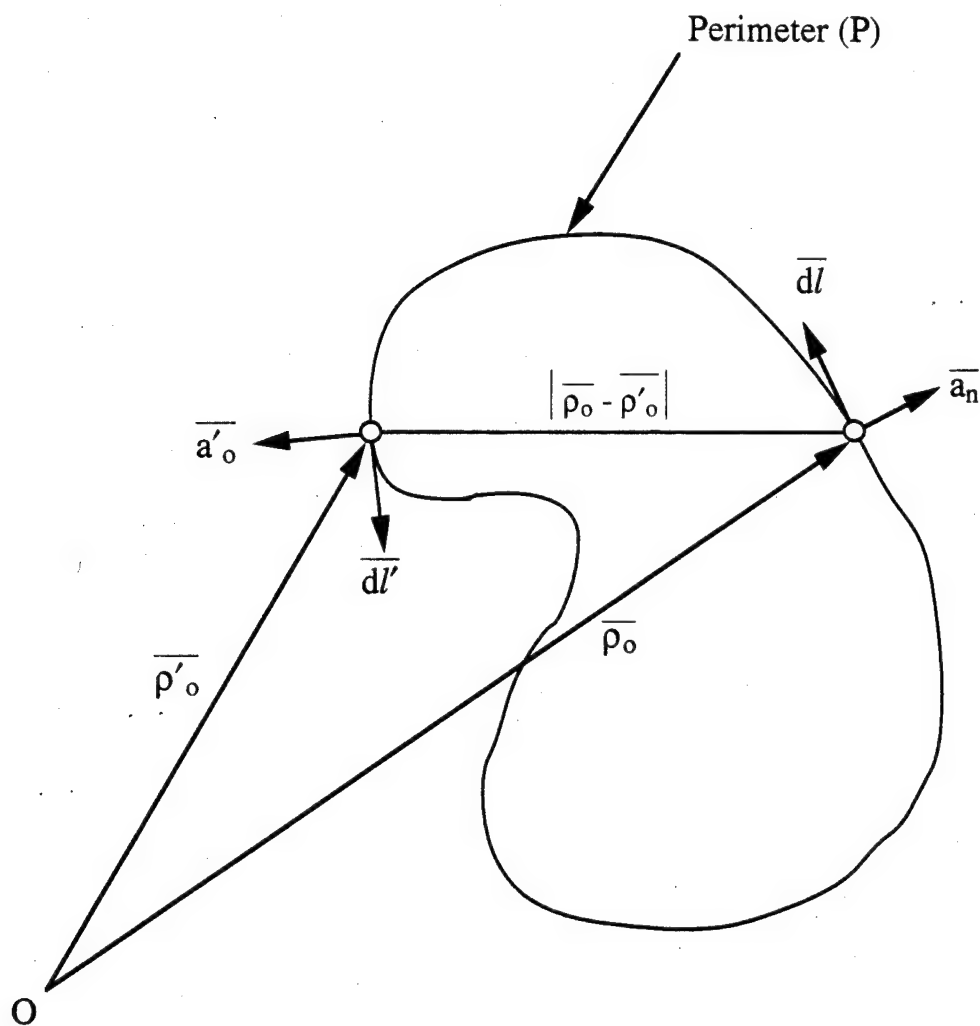
Figure A-9. Arrangement of variables used in computing the function $A_1(P)$ in (A-13a). From Kuester [18].

TABLE A-1

Comparison of Coaxial End-Effect Approximation

$$C_T \cong -2\pi\varepsilon b \left[\frac{ln(b/a)}{3+ln^3(b/a)} \right]$$

with Theory and Experiment

		Value of $-C_T$, Picofarads (pF)*		
b/a	b (inch)	Theory [27]	Approx.	Measured [28]
2.21	0.156	0.048	0.050	0.048
4.00	0.375	0.127	0.130	0.159
5.32	0.375	0.111	0.115	0.118
5.33	0.500	0.147	0.154	0.223
7.09	0.500	0.123	0.132	0.184
8.00	0.750	0.186	0.184	0.270
10.64	0.750	0.139	0.154	0.223
18.88	1.77	0.266	0.259	0.366
25.11	1.77	0.193	0.221	0.264

* With $\varepsilon_r = 1$.

TABLE A-2

Values of the Coefficient $A_1(P)$ used with Capacitance Approximation

$$C \cong \frac{\varepsilon_o \varepsilon_r S}{h} + \frac{\varepsilon_o P}{\pi}\left[1 + ln\left(\frac{2P}{\pi h}\right) + A_1(P) + \varepsilon_r A_2(\varepsilon_r) \right]$$

where

$$A_2(\varepsilon_r) \cong \frac{1}{2}\left(\frac{\varepsilon_r - 1}{\varepsilon_r}\right) ln\left[1 - 0.6735\left(\frac{\varepsilon_r - 1}{\varepsilon_r}\right) + 0.0788\left(\frac{\varepsilon_r - 1}{\varepsilon_r}\right)^2 \right] + ln\,(2\pi)$$

for Various Plate Geometries
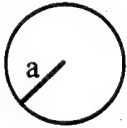
Plate shape	Perimeter (P)	Area (S)	$A_1(P)$
circle, radius a	$2\pi a$	πa^2	-2
triangle, side a	$3a$	$\dfrac{\sqrt{3}\,a^2}{4}$	-2.746
hexagon, side a	$6a$	$\dfrac{3\sqrt{3}\,a^2}{2}$	-2.185
rectangle, $2a \times a$	$6a$	$2a^2$	-2.279
square, side a	$4a$	a^2	-2.402

TABLE A-3

Effective radius (a_e) used with Capacitance Approximation

$$C \cong \frac{2\pi \varepsilon_o (\varepsilon_r + 1) a_e}{arctan \left[\frac{h B(\varepsilon_r)}{a_e} \right]}$$

where

$$B(\varepsilon_r) = \frac{\varepsilon_r - 1}{\varepsilon_r \ln \left(\frac{2\varepsilon_r}{\varepsilon_r + 1} \right)}$$

for Various Plate Geometries
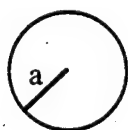
Plate shape	Effective radius, a_e
	a
	$\frac{\pi a}{K(k)}$, where $k = \sqrt{1 - (b/a)^2}$ and $$K(k) = \int_0^{\pi/2} \frac{d\theta}{\sqrt{1 - k^2 \sin^2 \theta}}$$
	0.7322a
	0.5765a
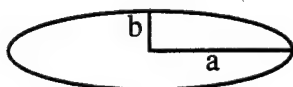
43
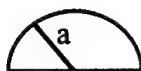
TABLE A-3 (Cont'd)
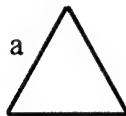
Plate shape	Effective radius, a_e
	0.3961a
	0.4364a
	0.2940a
	0.9149a
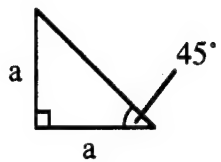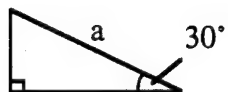
APPENDIX B

APPROXIMATION FOR THE RATIO OF THE COMPLETE ELLIPTIC INTEGRALS $K(k')/K(k)$

1. Background

The design or analysis of planar transmission lines, such as striplines or coplanar waveguides, frequently involves the computation of the ratio of complete elliptic integrals of the first kind, $K(k')/K(k)$ (often written simply as K'/K), where

$$K(k) = \int_0^{\pi/2} \frac{d\theta}{\sqrt{1-k^2\sin^2\theta}} \quad . \tag{B-1}$$

The argument k (the *modulus*), a function of the line parameters, numerically assumes a value between zero and one. The complementary modulus, k', is related to k by

$$k' = \sqrt{1 - k^2} \quad . \tag{B-2}$$

Expressions for the characteristic impedance (or alternatively, the per-unit-length capacitance or inductance) of planar transmission lines are derived by solving Laplace's equation in two dimensions using conformal mapping [39].

A plot of the ratio $K(k')/K(k)$ is shown in Fig. B-1 as a function of k (solid line). Also included in the figure are two curves (dotted lines) of the ratio in the limit of small ($k \to 0$) and large ($k \to 1$) moduli, given as [20]

$$\lim_{k \to 0} \left[\frac{K(k')}{K(k)} \right] \to \frac{2}{\pi} \ln\left(\frac{4}{k} \right) \tag{B-3a}$$

and

$$\lim_{k \to 1} \left[\frac{K(k')}{K(k)} \right] \to \frac{\pi}{2 \ln\left(\dfrac{4}{k'} \right)} \quad . \tag{B-3b}$$

The expression in (B-3b) is derived through exploitation of the ratio's antisymmetric behavior about the inflection point, at $k = 1/\sqrt{2}$. This amounts to the substitution of k' in place of k in the first expression (not proven here), followed by the use of

$$\frac{K(k')}{K(k)} = \frac{1}{K(k) / K(k')} \quad . \tag{B-3c}$$

Techniques for evaluating the ratio K(k')/K(k) are numerous and, depending on the application, may range from the classical methods employing theta functions [40], to numerical or iterative schemes [19, 41-42]. All of these methods are rather efficient when properly implemented on a computer. However, most of them use several expressions or repetitions thereof to cover the entire domain ($0 \leq k \leq 1$), making them unattractive for manual computation. The need for a simple and accurate expression, valid over the desired domain, was recognized. Moreover, the simplification of complicated analytical expressions in which the ratio K(k')/K(k) appears may be made through substitution of an accurate approximation. These two objectives provided the motivation to undertake this study.

2. Derivation of K(k')/K(k) approximation

2.1. Approach

To be useful, an approximation for K(k')/K(k) must yield accurate numerical values at three critical points along the domain:

Value of k	Value of K(k')/K(k)
0	∞
$1/\sqrt{2}$	1
1	0

A first approximation for K(k')/K(k) is derived by equating the approximate and exact formulas for the characteristic impedance of a transmission line. This method is similar to the one used by Hilberg [41-43]. An improvement in the accuracy of the first approximation is then made by adding another term to the function's argument, derived through the aid of a nonlinear regression scheme.

In contrast, Hilberg's method of improvement utilizes an iterative stereographic projection method to obtain a sequence of approximations for K(k')/K(k). This approach offers a very high degree of refinement, though not over the entire domain of interest. The approximations derived from Hilberg's method are suitable only in the domain spanning from the inflection point ($k = 1/\sqrt{2}$) to either end point ($k = 0$ or 1). The solutions for the remaining portion of the domain are found by interchanging k' and k, followed by the application of (B-3c).

46

2.2. First approximation

Consider a transmission line whose cross section comprises two thin opposing curved plates along a circle of diameter D and separated by a gap s, as shown in Fig. B-2. An approximate expression for the characteristic impedance of this line is given as [44]

$$Z_o \cong \frac{\pi}{4} \cdot \frac{\eta_o}{\operatorname{arccosh}\left[\cot\left(\frac{\theta}{2}\right)\right]} \quad , \quad \text{(ohms)} \tag{B-4}$$

where

$$\eta_o = \sqrt{\mu_o / \varepsilon_o} = \text{wave impedance of free space} \ (\cong 376.7 \text{ ohms }),$$

$$\mu_o = 4\pi \times 10^{-7} \text{ H/m} \ \text{(permeability of free space)},$$

$$\varepsilon_o \cong 8.854 \times 10^{-12} \text{ F/m} \ \text{(permittivity of free space)}.$$

The exact expression for the characteristic impedance of the same configuration is given as [43]

$$Z_o = \frac{\eta_o}{2} \cdot \frac{K(k)}{K(k')} \quad , \quad \text{(ohms)} \tag{B-5}$$

where the modulus $k = s/D = \sin \theta$. By equating (B-4) and (B-5) and noting that

$$\cot\left(\frac{\theta}{2}\right) = \frac{1 + \cos \theta}{\sin \theta} = \frac{1 + k'}{k} \quad ,$$

one obtains a first approximation for $K(k')/K(k)$, of the form

$$\frac{K(k')}{K(k)} \cong \frac{2}{\pi} \operatorname{arccosh}\left[\frac{1 + k'}{k}\right] \quad . \tag{B-6}$$

The accuracy of (B-6) was determined by comparing the value given by the right hand side with a precise value of $K(k')/K(k)$, computed with an accurate (relative error less than 2×10^{-8}) polynomial approximation for $K(k)$ [19]. The comparison revealed that (B-6) is accurate to within three significant figures for $k \le 0.2$. However, for $0.2 \le k \le 1$, (B-6) yields values that are smaller than those plotted in Fig. B-1, suggesting that the required argument must be larger than $(1+k')/k$ by some amount, to yield better accuracy.

2.3. Improvement of the first approximation

The domain over which (B-6) is valid can be considerably widened by adding a correction term in the argument, i.e., we let

$$\frac{K(k')}{K(k)} = \frac{2}{\pi} \operatorname{arccosh}\left[\frac{1+k'}{k} + \delta\right] .$$

Figure B-3 shows the value of δ (plotted against k', for clarity) required to yield the correct value of $K(k')/K(k)$ over the entire domain of $0 \le k \le 1$. The values of δ were computed by equating the left and right hand sides of the expression above, with $K(k')/K(k)$ obtained by numerical integration. The simplest approximation for δ, found by applying nonlinear regression, is given by

$$\delta \cong \frac{\sqrt[4]{k'}}{4} \cdot \sqrt{\frac{1-k'}{1+k'}} = \frac{k\sqrt[4]{k'}}{4(1+k')} .$$

The substitution of the above expression for δ into the postulated form for $K(k')/K(k)$ leads to the following final result:

$$\frac{K(k')}{K(k)} \cong \frac{2}{\pi} \operatorname{arccosh}\left[\frac{1+k'}{k} + \frac{k\sqrt[4]{k'}}{4(1+k')}\right] . \tag{B-7}$$

The table below compares (B-7) with the exact values at the critical points given earlier:

	Value of $K(k')/K(k)$	
Value of k	**Exact**	**From (B-7)**
0	∞	∞
$1/\sqrt{2}$	1	0.999 998
1	0	0

The relative error of (B-7) is shown in Fig. B-4. The curve was obtained through comparison of the value given by (B-7) with the exact value of $K(k')/K(k)$, obtained by numerical integration for $0.15 \le k \le 1$. The numerical integration results are accurate to within 10^{-13}.

3. Discussion of results

Figure B-4 indicates that the relative error of (B-7) is less than 2×10^{-4} for $0 \le k \le 0.99$. For $0.99 \le k \le 0.999$, the relative error increases in a somewhat oscillatory fashion, reaching 3.5×10^{-3} at $k = 0.999$. For $k \ge 0.999$, the relative error increases further but quickly drops to zero when $k = 1$. An understanding of the behavior of (B-7) in the region $0.999 \le k \le 1$ can be facilitated with the observations that follow.

In the limit of large moduli, (B-7) reduces to the following form:

$$\lim_{k \to 1} \left\{ \frac{2}{\pi} \operatorname{arccosh}\left[\frac{1+k'}{k} + \frac{k\sqrt[4]{k'}}{4(1+k')} \right] \right\} \to \frac{\sqrt[8]{16\,k'}}{\pi} \ . \qquad \text{(B-8a)}$$

In contrast, from (B-3b),

$$\lim_{k \to 1} \left[\frac{K(k')}{K(k)} \right] \to \frac{\pi}{2\ln\left(\dfrac{4}{k'}\right)} \ . \qquad \text{(B-8b)}$$

Both (B-8a) and (B-8b) numerically approach zero as $k \to 1$ and are slowly varying in that region. In order to clearly distinguish the error incurred by the use of (B-7), it is useful to compute the ratio of the values of (B-8a) and (B-8b). In doing so, one obtains the following result:

$$F(k') = \frac{\text{Eq. (B-8a)}}{\text{Eq. (B-8b)}} = \frac{2}{\pi^2} \sqrt[8]{16\,k'}\ \ln\left(\frac{4}{k'}\right) \ . \qquad \text{(B-9)}$$

A plot of (B-9) is shown in Fig. B-5. From the figure, it can be seen that (B-7) is slightly larger than (B-3b) at $\log_{10}(k') \cong -2.87$ ($k' \cong 1.34 \times 10^{-3}$) and is smaller elsewhere. Table B-1 shows how (B-7) compares with the exact values of $K(k')/K(k)$, for moduli very close to unity.

As shown in Table B-1, approximation (B-7) is smaller in value than the exact result, accounting for the rapid increase in error. In practical work, however, values of k such as shown in the table are uncommon. Although it can be argued that (B-3b) can be used to rigorously extend the allowable range of k, it is not necessary. In general, transmission line parameters derived from such near-unity moduli may be either too small or too large to be useful in practical applications. Therefore, (B-7) is an expression that may be used for most practical computations.
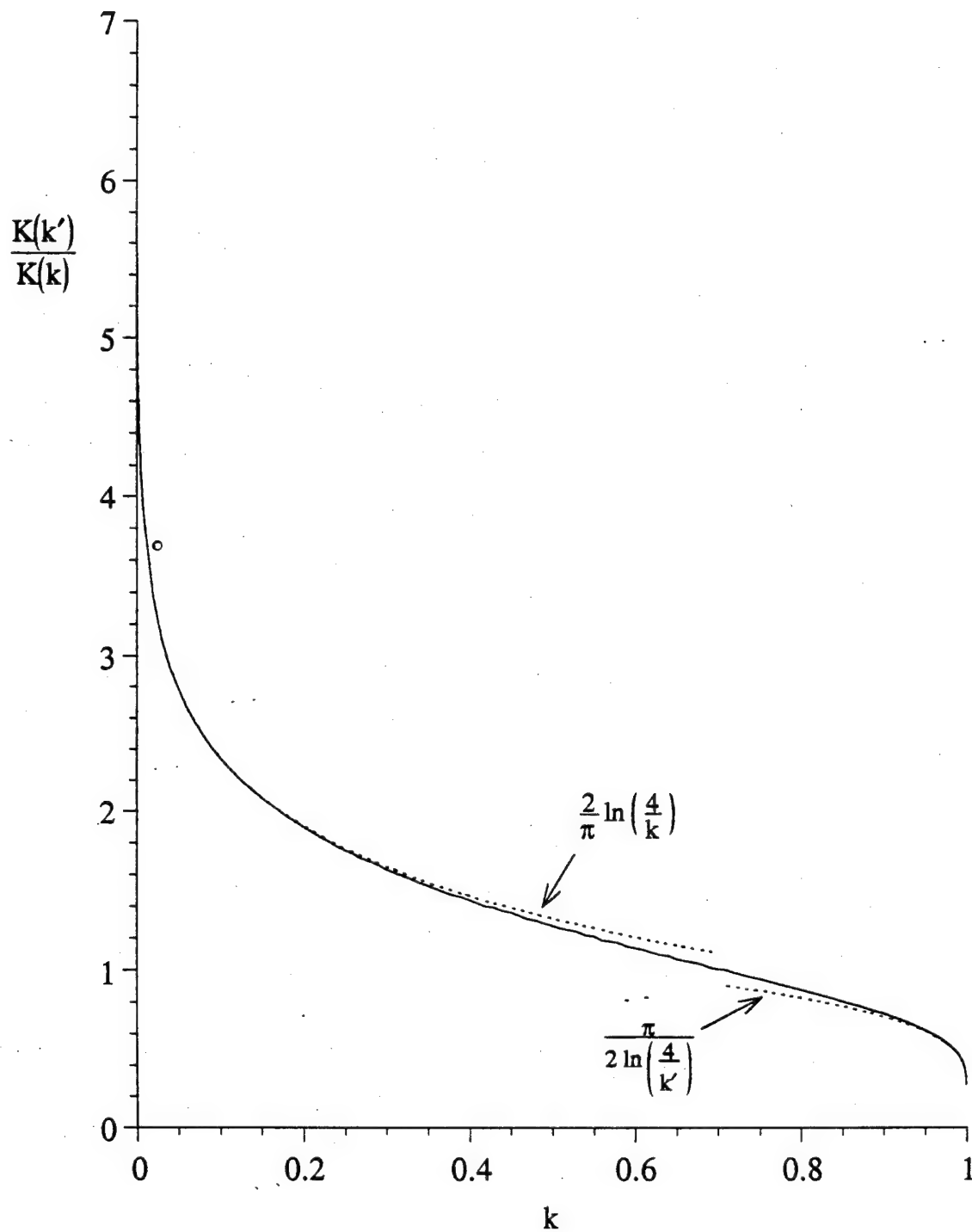
Figure B-1. Ratio of the complete elliptic integrals of the first kind, K(k′)/K(k); solid line. Shown in dotted lines are the limiting values of K(k′)/K(k), obtained from (B-3).
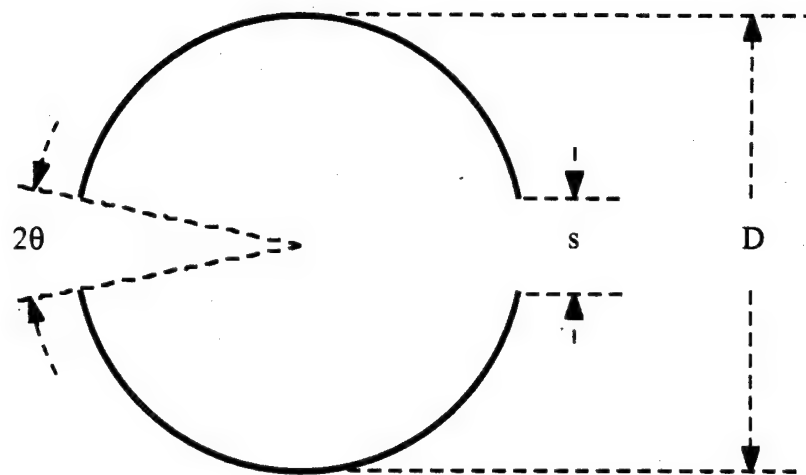
Figure B-2. Cross section of a curved plate transmission line used to
derive the first approximation, (B-6). The angular
separation, θ, is related to s and D by $\sin\theta = s/D$.

$$\frac{K(k')}{K(k)} = \frac{2}{\pi} \text{arccosh} \left[\frac{1+k'}{k} + \delta \right]$$
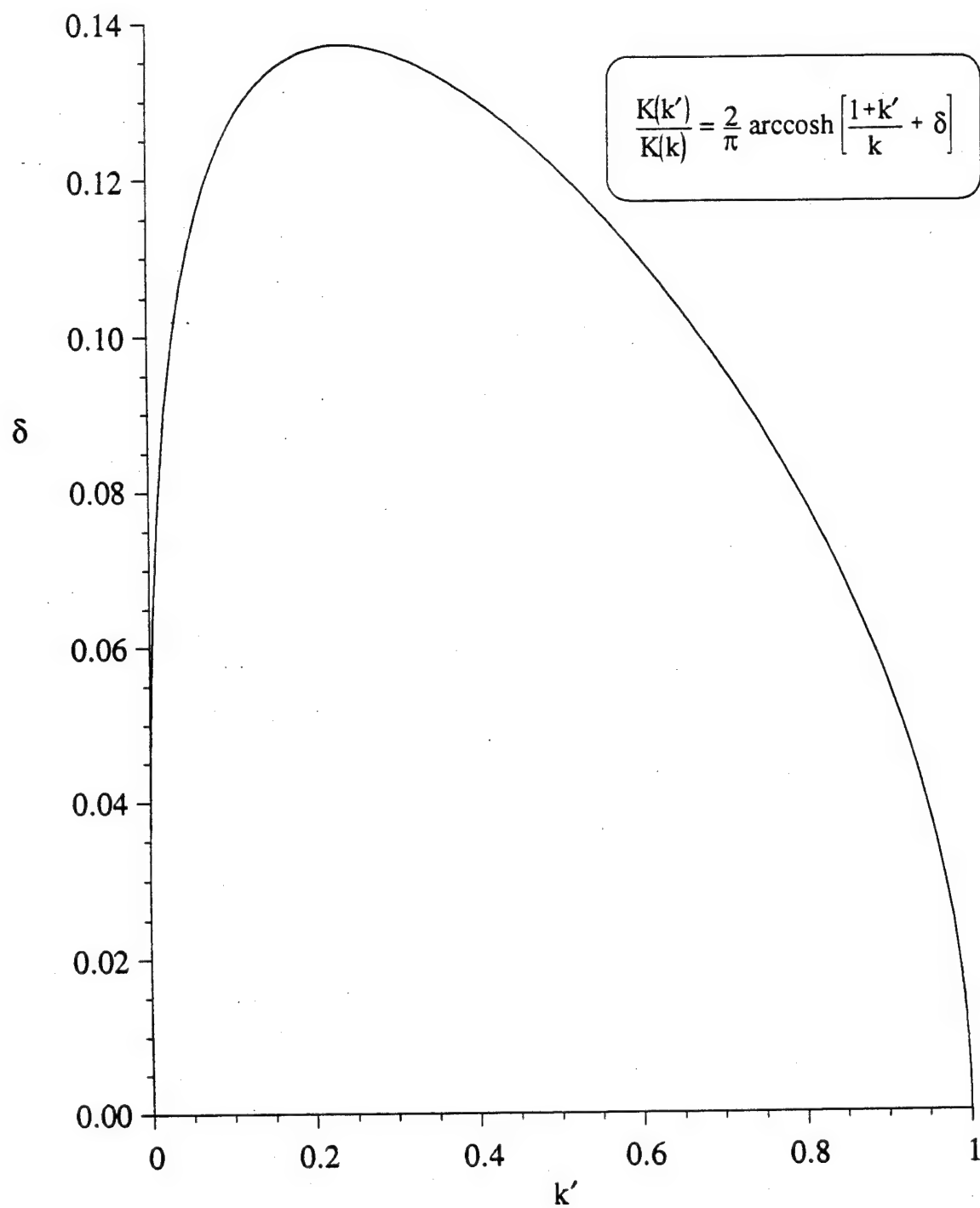
Figure B-3. Value of δ required to yield correct values of $K(k')/K(k)$.

$$\frac{K(k')}{K(k)} \cong \frac{2}{\pi} \text{arccosh}\left[\frac{1 + k'}{k} + \frac{k \sqrt[4]{k'}}{4(1 + k')}\right]$$
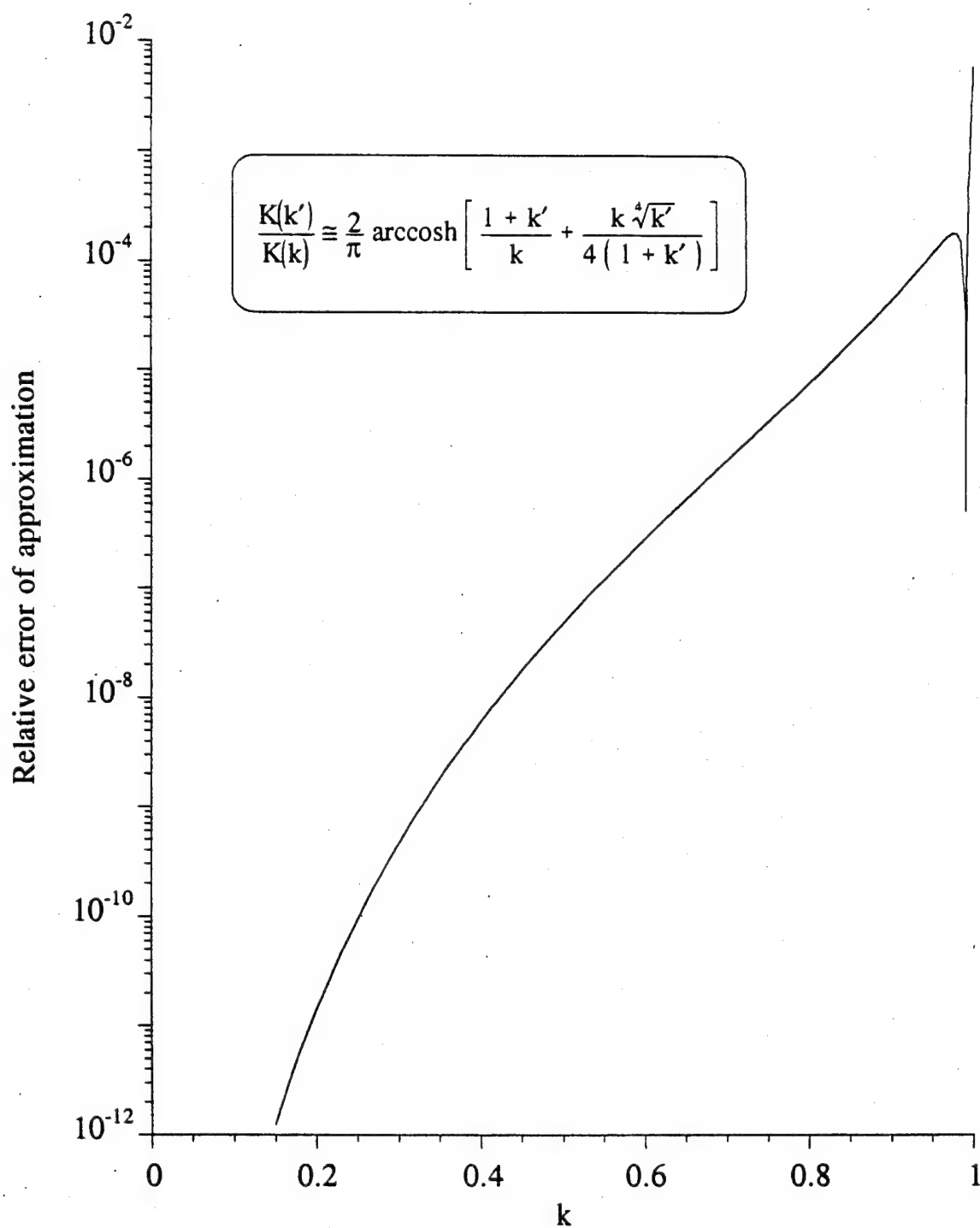
Figure B-4. Relative error incurred in computing $K(k')/K(k)$, using (B-7).

$$F(k') = \frac{2}{\pi^2} \sqrt[8]{16 \, k'} \, \ln\left(\frac{4}{k'}\right)$$

$k \cong 1 - \left(5 \times 10^{-41}\right)$

$k \cong 1 - \left(5 \times 10^{-5}\right)$
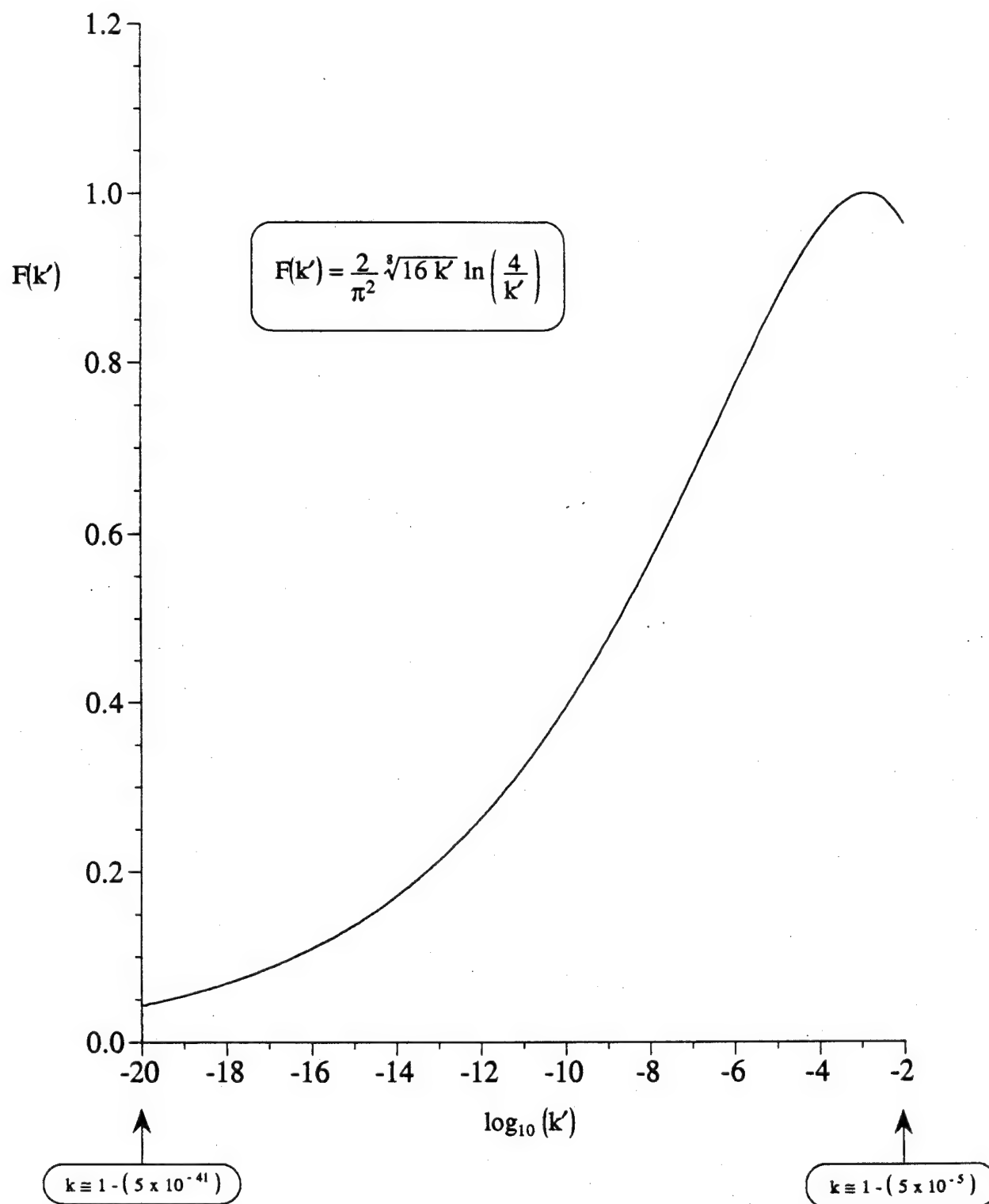
Figure B-5. Value of (B-7) relative to (B-3b) in the region of poorest accuracy (k→1).

TABLE B-1

Comparison of the Approximation

$$\frac{K(k')}{K(k)} \cong \frac{2}{\pi} \, arccosh \left[\frac{1 + k'}{k} + \frac{k \sqrt[4]{k'}}{4 \left(1 + k' \right)} \right]$$

with Exact Values, for Modulus k Close to Unity

		Value of K(k')/K(k)	
Value of k'	Value of k	Exact	Approx.
10^{-2}	0.999 950	0.262 172	0.265 632
10^{-4}	0.999 999 995	0.148 235	0.142 333
10^{-6}	$1 - (5 \times 10^{-13})$	0.103 330	0.080 003
10^{-8}	$1 - (5 \times 10^{-17})$	0.079 305	0.045 007
10^{-10}	$1 - (5 \times 10^{-21})$	0.064 345	0.025 312
...	...	...	...
0	1	0	0

APPENDIX C

NUMERICAL CONVERGENCE OF THE
METHOD OF MOMENTS ALGORITHM

1. Introduction

The method of moments code that was used in this investigation is based on the solution of the potential integral equation (3) for the unknown charge density $q(z)$. The details of this program are provided in [15]. Because the method of moments data are used as a basis for evaluation of the capacitance formulas presented in this report, it is important that a sufficient number of basis functions are used in order to insure convergence of the tubular monopole capacitance to a given number of significant figures. This concern prompted a detailed numerical study of the condition(s) required to insure convergence. This appendix provides a summary of this study.

2. Results

Convergence tests were performed to determine the required number of basis functions for different ranges of $\log_{10}(D)$ and $\log_{10}(H)$. Figure C-1 shows the normalized capacitance as a function of the number of basis functions for the case $\log_{10}(D) = 0$ and $\log_{10}(H) = -1$. The graph indicates that the data converges to three significant figures with less than 1500 basis functions. Figure C-2 illustrates a similar plot for the same thickness tube with $\log_{10}(H) = -3$. In this case, approximately 2500 basis functions are required before convergence to three significant figures is attained. In general, the convergence of the tubular monopole capacitance was found to be slower both for thicker tubes and for smaller separations above the ground plane.

Figure C-3 shows the number of basis functions used in the method of moments algorithm for different ranges of tube thicknesses and separations above the ground plane. The basis functions listed in Fig. C-3 provide convergence to at least three significant figures. Because of the variability in convergence with tube thickness, Fig. C-3 is divided into three regions, i.e., thin, medium, and fat. Since the convergence of the tubular monopole capacitance slows considerably for $\log_{10}(H) < -3$, the number of basis functions N used in this report is given as a linear function of $\log_{10}(H)$ for each tube-thickness region. In the thin-tube region ($-3 \leq \log_{10}(D) \leq -2$), we have

$$N = 1900 - 6200 \left[\log_{10}(H) + 3.5 \right] , \quad -4 \leq \log_{10}(H) \leq -3.5 . \qquad (C-1)$$

Similarly, in the medium-tube region ($-2 < \log_{10}(D) < 0$), the number of basis functions is given

by

$$N = 1900 - 4100 \left[\log_{10}(H) + 3 \right] , \quad -4 \le \log_{10}(H) \le -3 , \qquad (C\text{-}2)$$

while in the fat-tube region $(0 \le \log_{10}(D) \le 3)$, we have

$$N = 2500 - 5500 \left[\log_{10}(H) + 3 \right] , \quad -4 \le \log_{10}(H) \le -3 . \qquad (C\text{-}3)$$

Note that at the smallest ground-plane separation (i.e., $\log_{10}(H) = -4$), 5000 basis functions are required for a thin tube in contrast to 8000 basis functions for a fat tube.

As an additional check of the algorithm, the moment-method capacitance data was examined for tubular monopoles of different radii as a function of the height above the ground plane. Figures C-4 and C-5 provide plots of the normalized capacitance as a function of $\log_{10}(H)$ for $\log_{10}(D) = -1$ and $\log_{10}(D) = 3$, respectively. In both cases, the curves show that the capacitance increases almost linearly with decreasing $\log_{10}(H)$. Monopoles of different diameters were observed to exhibit a similar behavior.
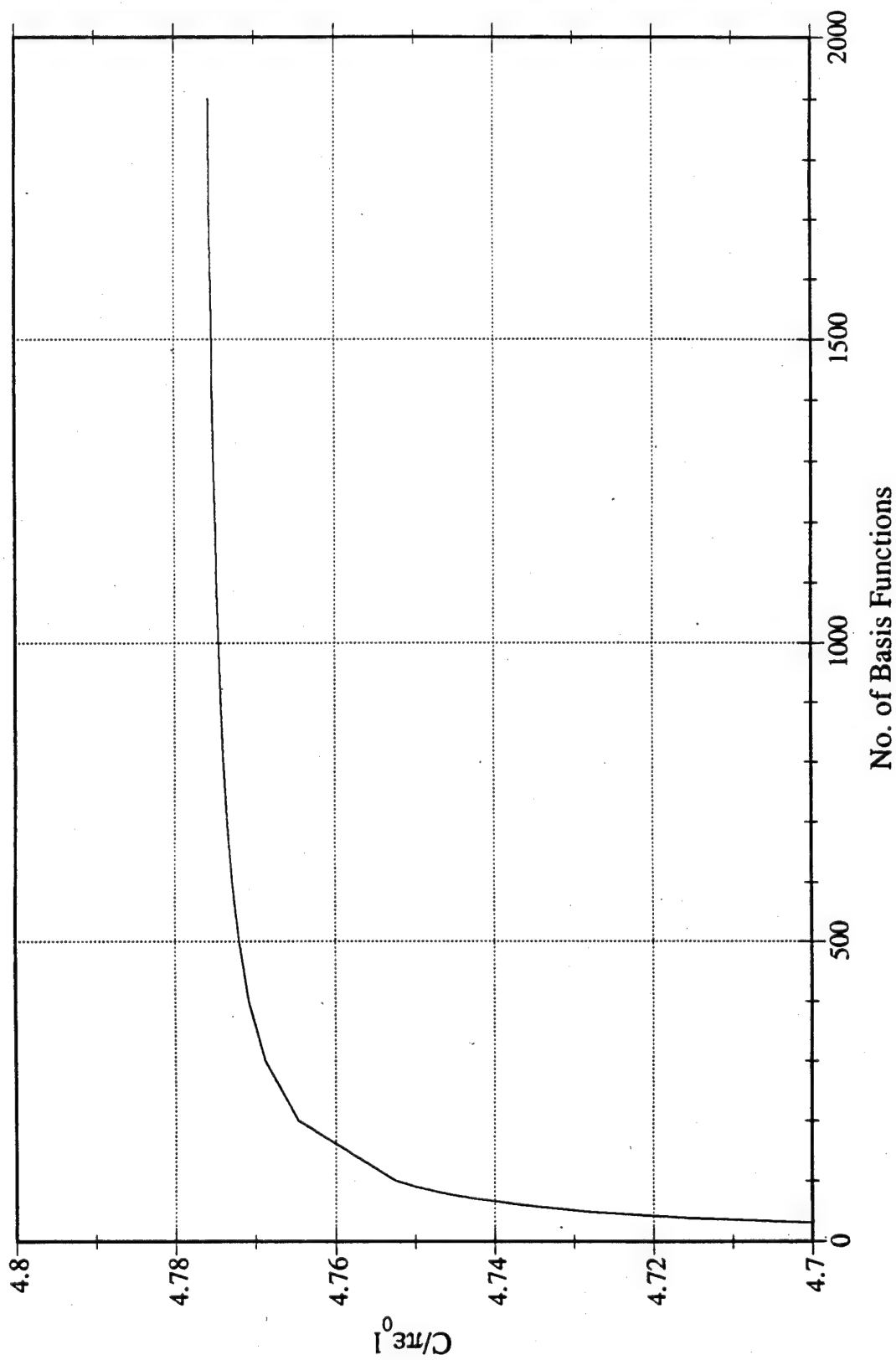
Figure C-1. Normalized capacitance of a tubular monopole versus the number of basis functions for $\log_{10}(D) = 0$ and $\log_{10}(H) = -1$ as determined by the method of moments algorithm.
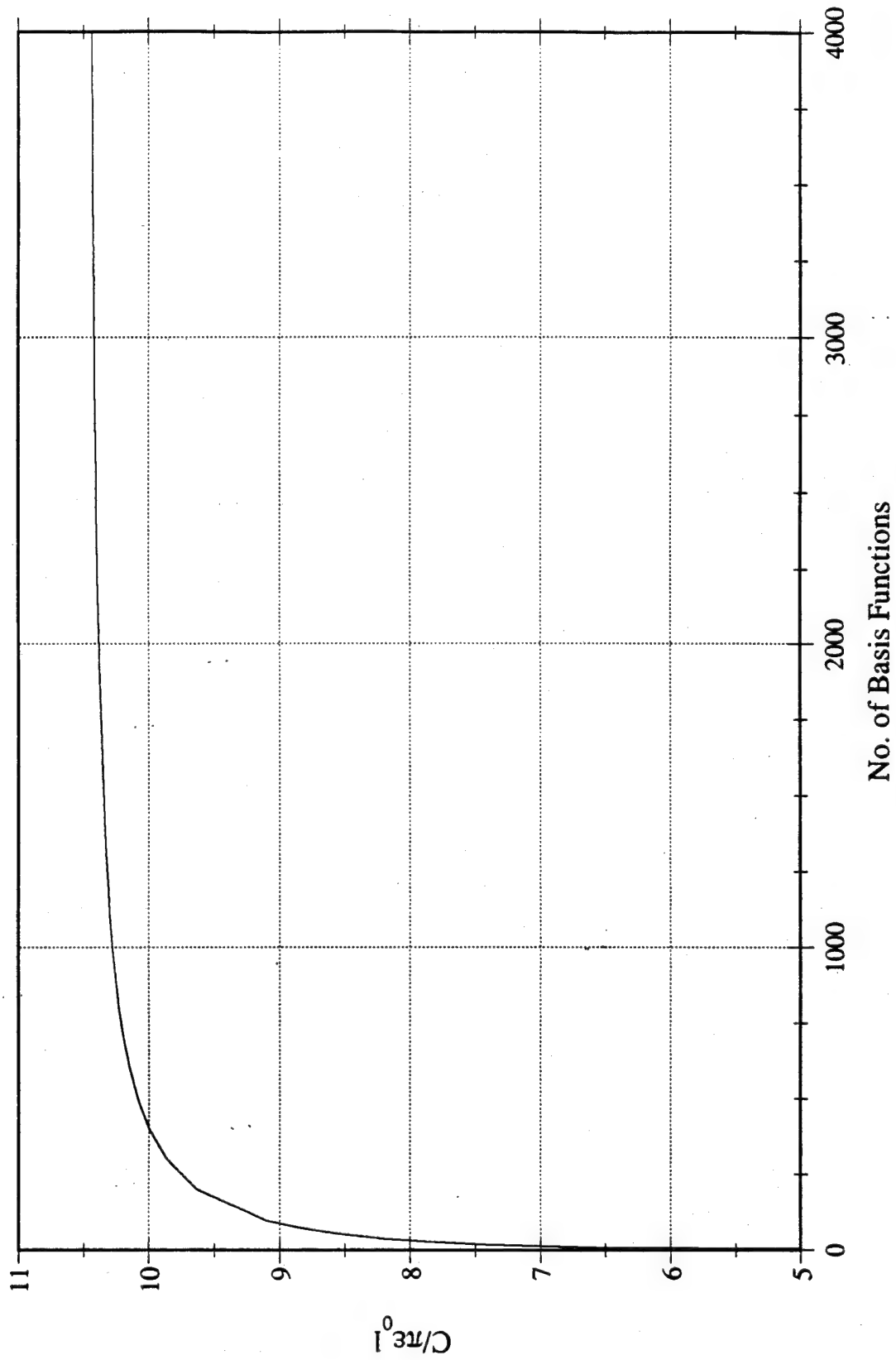
Figure C-2. Normalized capacitance of a tubular monopole versus the number of basis functions for $\log_{10}(D) = 0$ and $\log_{10}(H) = -3$ as determined by the method of moments algorithm.
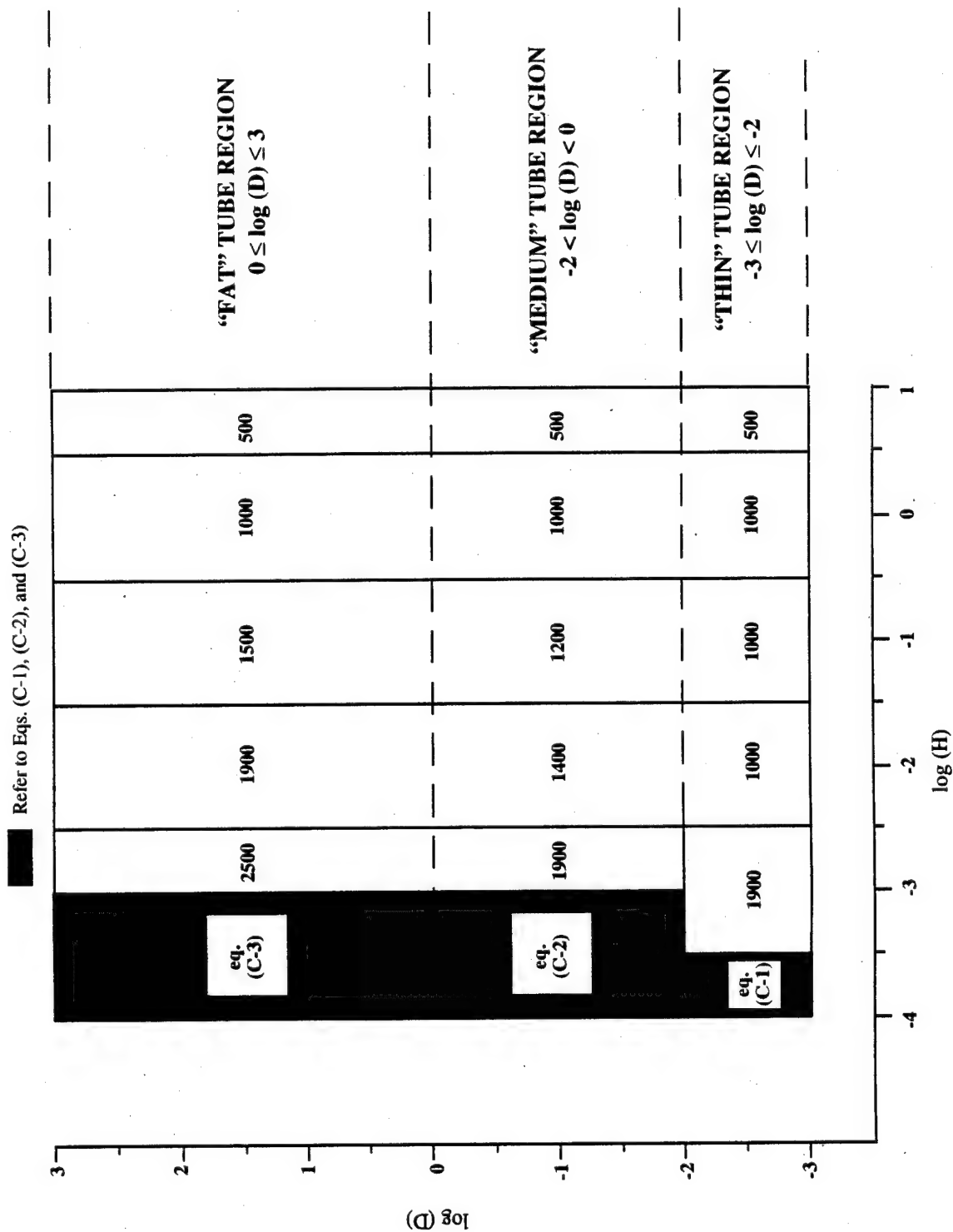
Figure C-3. Number of basis functions required to insure a minimum of three significant figure accuracy in the method of moments algorithm used for computing tubular monopole capacitance.
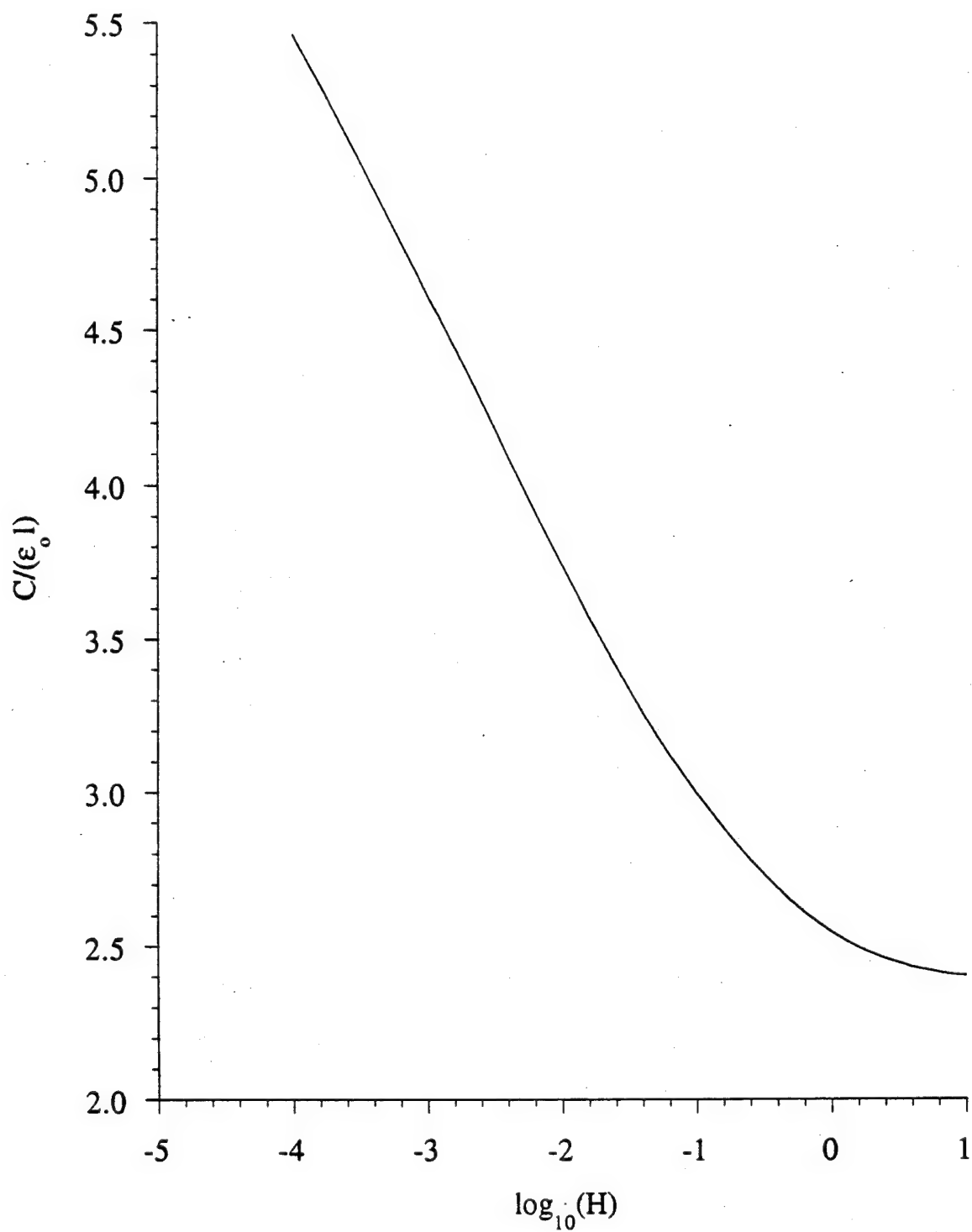
Figure C-4. Variation of the normalized tubular monopole capacitance with height for $\log_{10}(D) = -1$.
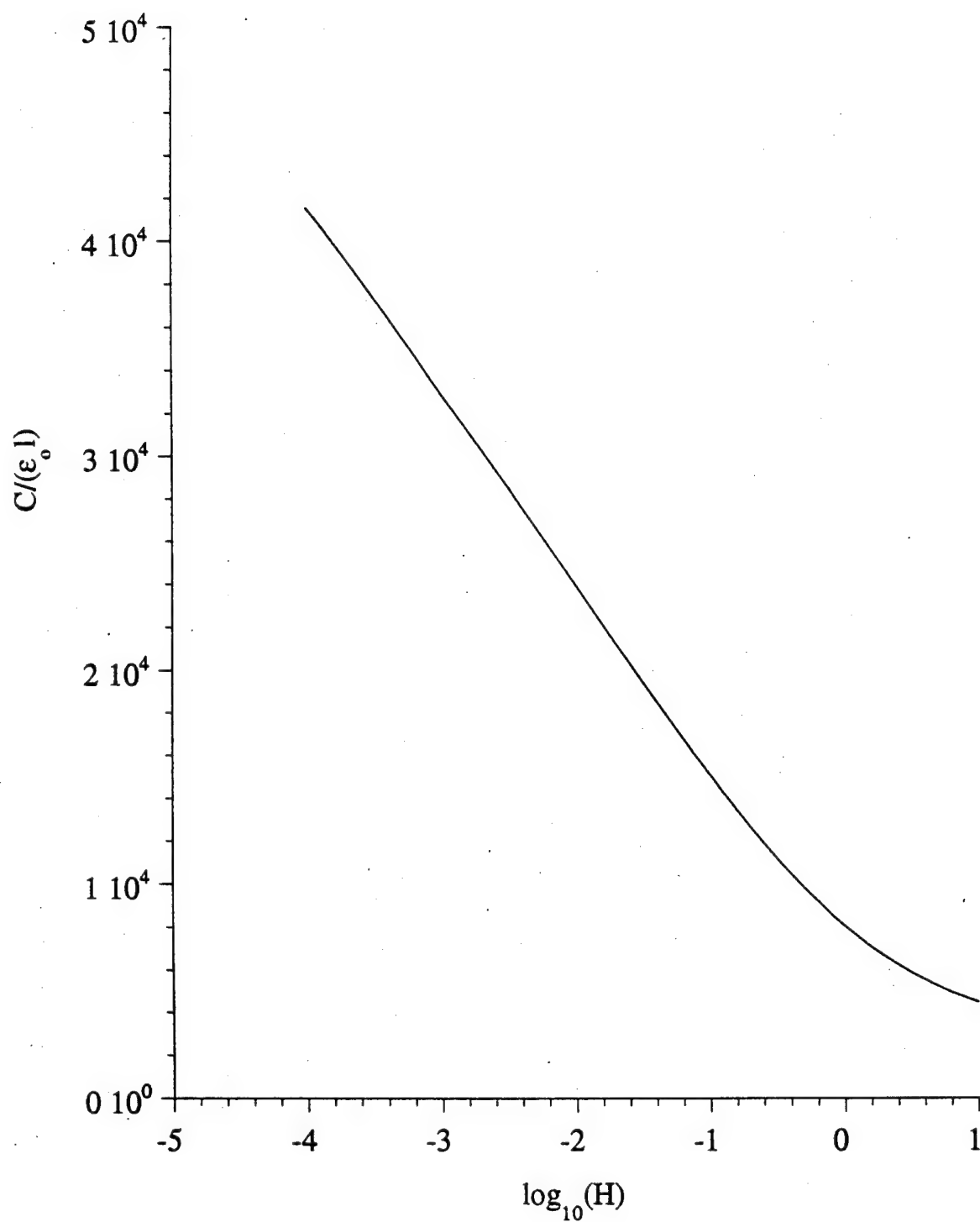
Figure C-5. Variation of the normalized tubular monopole capacitance with height for $\log_{10}(D) = 3$.

REFERENCES

[1] Schelkunoff, S. A. and H. T. Friis, **Antennas: Theory and Practice**. (New York: John Wiley & Sons, 1952), chapter 10.

[2] Hagaman, B. G., "Low Frequency Antennas" in **Antenna Engineering Handbook, 2nd ed.** (New York: McGraw-Hill, 1984), chapter 24.

[3] Belrose, J. S., "VLF, LF and MF Antennas" in **The Handbook of Antenna Design, Vol. 2.** (London: Peter Perigrinus Ltd., 1983), chapter 15.

[4] Leonhard, J., R. D. Mattuck, and A. J. Poté, "Folded Unipole Antennas", *IRE Transactions on Antennas and Propagation*, (3) **1955**, pp. 111-116.

[5] Harrison, C. W. and R. W. P. King, "Folded Dipoles and Loops", *IRE Transactions on Antennas and Propagation*, (9) **1961**, pp. 171-187.

[6] Gangi, A. F., S. Sensiper, and G. R. Dunn, "The Characteristics of Electrically Short Umbrella Top-Loaded Antennas", *IEEE Transactions on Antennas and Propagation*, (13) **1965**, pp. 864-871.

[7] Seely, E. W., "An Experimental Study of the Disk-Loaded Folded Monopole", *IRE Transactions on Antennas and Propagation*, (4) **1956**, pp. 27-28.

[8] Devaney, T. E., R. F. Hall, and W. E. Gustafson, "Low-Frequency Top Loaded Antennas", U. S. Navy Electronics Laboratory, NEL Report 1381, 22 June 1966, p. 10.

[9] Watt, A. D., **VLF Radio Engineering.** (Oxford: Pergamon Press, 1967), chapter 2.

[10] Harrington, R. F., **Field Computation by Moment Methods.** (Malabar, FL: R. E. Krieger Publishing Co.,1982).

[11] Grover, F. W., "Methods, Formulas, and Tables for the Calculation of Antenna Capacity", *Bureau of Standards Scientific Papers* (22) **1926**. Paper No. 568, pp. 569-629.

[12] Howe, G. W. O., "On the Capacity of Radio-Telegraphic Antennae", *The Electrician* (73) **1914**, pp. 829-832, 859-864, 906-909.

[13] Casey, J. P. and R. Bansal, "Capacitance of a Small Tubular Antenna", *Electronics Letters* (24) **1988**, pp. 1021-1022.

[14] Hanna, V. F., "Finite Boundary Corrections to Coplanar Stripline Analysis", *Electronics Letters*, (16) **1980**, pp. 604-606.

[15] Casey, J. P. and R. Bansal, "Analysis and Design of a Loran-C Antenna", NUSC Technical Report 8643, Naval Underwater Systems Center, New London, CT, 18 October 1989.

[16] King, R. W. P., H. R. Mimno, and A. H. Wing, **Transmission Lines, Antennas, and Waveguides.** (New York: Dover Publications; rpt., 1965), chapter II.

[17]   Wilton, D. R., "Static Analysis of Conical Antenna Over a Ground Plane", University of Mississippi, AFOSR-TR-76-1078, Air Force Office of Scientific Research, Bolling AFB, Washington, D.C., August, 1976.

[18]   Kuester, E. F., "Explicit Approximations for the Static Capacitance of a Microstrip Patch of Arbitrary Shape", *Journal of Electromagnetic Waves and Applications*, (**2**) **1987**, pp. 103 - 135.

[19]   Abramowitz, M and I. A. Stegun, eds. **Handbook of Mathematical Formulas, Graphs and Mathematical Tables [National Bureau of Standards Applied Mathematics Series, No. 55].** (Washington, D.C.: U. S. Dept. of Commerce, 1967), chapter 17.

[20]   Bowman, F. **Introduction to Elliptic Functions with Applications.** (New York: John Wiley & Sons, 1953), chapter II.

[21]   Butler, C. M., "Capacitance of a Finite-Length Conducting Cylindrical Tube", *Journal of Applied Physics*, (**51**) **1980**, pp. 5607 - 5609.

[22]   Hallén, E., "Theoretical Investigations into Transmitting and Receiving Antennae", *Nova Acta Regiae Soc. Sci. Upsaliensis*, Ser. IV, (**11**) **1938**, pp. 1 - 44.

[23]   Lo, Y. T., "A Note on the Cylindrical Antenna of Noncircular Cross Section", *Journal of Applied Physics,* (**24**) **1953** pp. 1338-1339.

[24]   Su, C. W. H. and J. P. German, "The Equivalent Radius of Noncircular Antennas", *Microwave Journal,* (**9**) **1966**, pp. 64-67.

[25]   Jaggard, D. L., "On Bounding the Equivalent Radius", *IEEE Transactions on Antennas and Propagation,* (**28**) **1980**, pp. 384-388.

[26]   Cohn, S.B., "Thickness Corrections for Capacitive Obstacles and Strip Conductors," *IRE Trans. Microwave Theory and Techniques,* (**8**) **1960**, pp. 638-644.

[27]   King, R. (W.P.), "The End Correction for a Coaxial Line When Driving an Antenna over a Ground Screen," *IRE Trans. Antennas and Propagation,* (**3**) **1955**, pp. 66-72.

[28]   Hartig, E.O., "Circular Apertures and Their Effects on Half-Dipole Impedances," Cruft Lab. Tech. Rep. No. 107, June 1950.

[29]   Schelkunoff, S.A., "Theory of Antennas of Arbitrary Size and Shape," *Proceedings of the IRE,* (**29**) **1941**, pp. 493-521.

[30]   Kuester, E.F., "Accurate Approximations for a Function Appearing in the Analysis of Microstrip," *IEEE Trans. Microwave Theory and Techniques,* (**32**) **1984**, pp. 131-133.

[31]   Reitan, D.K. and T.J. Higgins., "Accurate Determination of the Capacitance of a Thin Rectangular Plate," *Trans. AIEE*, pt. I, Communications and Electronics, (**75**) **1956**, pp.761-766.

[32]   De Meulenaere, F. and J. Van Bladel., "Polarizability of some small apertures," *IEEE Trans. Antennas and Propagation,* (**25**) **1977**, pp. 198-205.

[33] Fuller, J.A. and D.C. Chang., "On the Numerical Calculation of Capacitance in the Presence of Edge Boundaries," *Proc. IEEE*, (58) **1970**, pp. 490-491.

[34] Ruehl, A.E. and P.A. Brennan., "Efficient Capacitance Calculations for Three-Dimensional Multiconductor Systems," *IEEE Trans. Microwave Theory and Techniques,* (21) **1973**, pp. 76-82.

[35] Balaban, P., "Calculation of Capacitance Coefficients of Planar Conductors on a Dielectric Surface," *IEEE Trans. Circuit Theory,* (20) **1973**, pp. 725-731.

[36] Okon, E.E. and R.F. Harrington., "A Method of Computing the Capacitance of Flat disks of Arbitrary Shape," *Electromagnetics*, (1) **1981**, pp. 229-241.

[37] Pólya, G., and G. Szegö. **Isoperimetric Inequalities in Mathematical Physics.** (Princeton: Princeton University Press, 1951).

[38] Fabrikant, V.I., "On The Capacity of Flat Laminae," *Electromagnetics*, (6) **1986**, pp. 117-128.

[39] Ramo, S., Whinnery, J.R. and T. Van Duzer. **Fields and Waves in Communication Electronics, 2nd ed.** (New York: John Wiley & Sons, 1984), chapter 7.

[40] Janke, E. and F. Emde. **Tables of Higher Functions, 5th ed.** (Leipzig: B.G. Teubner, 1952), chapter V.

[41] Hilberg, W., "From Approximations to Exact Relations for Characteristic Impedances," *IEEE Trans. on Microwave Theory and Techniques* **17 (1969)**, pp. 259-265.

[42] -------------., "Näherungen für die elliptische Integral-Funktion K/K′ und Rekursionen zur beliebigen Verbesserung ihrer Genauigkeit, insbesondere zur Wellenwiderstandsberechnung," *Arch. für Elektrotech.* **53 (1970)**, pp. 290-298.

[43] Hilberg, W. **Electrical Characteristics of Transmission Lines.** (Dedham, MA: Artech, 1979), chapter IV.

[44] International Telephone and Telegraph Corporation. **Reference Data for Radio Engineers, 4th ed.** (New York: ITT Corp., 1962), chapter 20.

INITIAL DISTRIBUTION LIST

Addressee	No. of Copies
Dr. Rajeev Bansal, University of Connecticut, Dept. of Electrical and Systems Enginnering U-157, Storrs, CT 06269	1
Dr. John S. Belrose, Communications Research Centre, 3701 Carling Ave., PO Box 11490, Sta. H, Ottawa, Ontario, Canada K2K 8S2	1
Dr. Chalmers M. Butler, Clemson University, Dept. of Electrical and Computer Engineering, Clemson, SC 29634	1
James Clark, USA-CRREL, 72 Lime Rd., Hanover, NH 03755-1290	1
DTIC, 8725 John J. Kingman Rd., Suite 0944, Fort Belvoir, VA 22060-6218	1
Dr. Kyohei Fujimoto, Tsukuba University, Institute of Applied Physics, Tsukuba, Japan	1
Dr. Robert C. Hansen, Box 570215, Tarzana, CA 91357	1
Dr. Ann Henderson, Royal Military College of Science, School of Electrical Engineering and Science, Shrivenham, Swindon Wilts, United Kingdom	1
Dr. Kazuhiro Hirasawa, Tsukuba University, Institute of Applied Physics, Tsukuba, Japan	1
Dr. James R. James, Royal Military College of Science, School of Electrical Engineering and Science, Shrivenham, Swindon Wilts, United Kingdom	1
Dr. R.W.P. King, Harvard University, Gordon McKay Lab, 9 Oxford St., Cambridge, MA 02138	1

INITIAL DISTRIBUTION LIST (Cont'd)

Addressee   **No. of Copies**

Addressee	No. of Copies
Dr. A. Kumar, AK Electromagnetic, Inc., 492 Westminster Ave., Dollard-des-Ormeaux, Quebec, Canada H9G 1E5	1
Dr. Donald Miller 13 Greentree Dr. East Lyme, CT 06333	1
Dr. Tapan Sarkar, Syracuse University, Dept. of Electrical Engineering, Syracuse, NY 13244	1
Dr. Harvey Schuman, Computer Sciences Corporation, P.O. Box 4308, Rome, NY 13442-4308	1
Gabriel Silberman, ARDEC, SCMAR-FSP-E, Bldg. 1530, Picatinny Arsenal, Picatinny, NJ 07806-5000	1
Valentin Trainotti, Carlos Calvo 665, 1° B, Buenos Aires, Argentina	1
Dr. Harold A. Wheeler, 4516 Atascadero Dr., Santa Barbara, CA 93110	1
Dr. Donald Wilton, University of Houston, Dept. of Electrical Engineering, Houston, TX, 77004	1
Dr. A.D. Wunsch, University of Lowell, Dept. of Electrical Engineering, Lowell, MA 01834	1